Density of pure and mixed NaCl and CaCl2 aqueous solutions at 293 K to 353 K and 0.1 MPa: an integrated comparison of analytical and numerical data

Ulrike Hoffert, Laurent André, Guido Blöcher, Sylvain Guignot, Arnault Lassin, Harald Milsch, Ingo Sass

Geothermal Energy

RESEARCH

Open Access

Density of pure and mixed NaCl and $CaCl_2$ aqueous solutions at 293 K to 353 K and 0.1 MPa: an integrated comparison of analytical and numerical data

Ulrike Hoffert[1*], Laurent André[2,3], Guido Blöcher[1], Sylvain Guignot[2], Arnault Lassin[2], Harald Milsch[1] and Ingo Sass[1]

*Correspondence:
hoffert@gfz-potsdam.de

[1] GFZ German Research Centre for Geosciences, Telegrafenberg, 14473 Potsdam, Germany
[2] BRGM, 3 Avenue Claude Guillemin, 45060 Orléans, France
[3] ISTO, UMR 7327, Université d'Orléans, CNRS, BRGM, OSUC, 45071 Orléans, France

Abstract

This study reports on newly acquired density data of synthetically prepared pure and mixed NaCl and $CaCl_2$ aqueous solutions that span a wide range of geothermally encountered concentrations and mixing ratios. The analytical data are provided for the temperature range of 293–353 K at ambient pressure. For the reproduction of that data, PHREESCALE was used. The predictive potential of this numerical tool regarding the density of geothermal fluids of known composition was the major target herein. As a result, the measured data are in good agreement with previous analytical studies found in the literature. Possible sources of errors are discussed in this paper. Density data of the mixed solutions at temperatures other than ambient are unique and close existing data gaps. The numerical model reproduces the newly measured and already existing density data within an error band of approximately 1%. For further use in geothermal applications, this can be considered an excellent agreement. Moreover, the model yields a direct calculation of density without the need to establish complex empirical equations of state and mixing rules. Finally, sensitivity calculations performed with a thermal–hydraulic (TH) numerical reservoir model demonstrate the required accuracy of fluid density for reliably predicting the long-term performance of deep geothermal energy systems. In terms of the productivity index and the timing of thermal breakthrough it shows that the present analytical and numerical uncertainty in density is small enough to reliably state both reservoir parameters.

Keywords: Density, Geothermal fluid, Sodium chloride, Calcium chloride, Geothermal energy

Introduction

The density of aqueous electrolyte solutions is of interest in a wide range of industrial, geotechnical and geoscientific applications. This particularly applies to geothermal technology development where the knowledge of the specific fluid density is required throughout the value chain, from reservoir exploration to energy production. This applies to all deep geothermal systems, not only those in sedimentary basins but also

the ones to be developed in the crystalline basement (e.g., *GeoLaB*; https://www.geolab.kit.edu/english/index.php). For example, fluid density controls the effective stress state of a reservoir via the hydrostatic pore pressure (e.g., Guéguen and Palciauskas 1994) and its knowledge is required for the evaluation of seismic exploration data (e.g., Mavko et al. 2009). Moreover, density influences fluid flow, both, within the reservoir and the wells (e.g., Bear 1988) and it impacts drilling operations as well as wellbore stability (e.g., Ahmed 2010). Not least, accurate density information is fundamental for the design and calibration of various components within the geothermal power plant, including pumps, heat exchangers, and separators (Francke and Thorade 2010; Frick et al. 2011).

The chemical properties of geothermal fluids in particular reservoirs are determined by their origin, the respective rock types and their stratigraphic correlation, the hydrogeological reservoir conditions, the formation depth and temperature as well as fluid age (e.g., Bethke et al. 1988; Nicholson 1993; Hanor 1994; Raffensperger and Vlassopoulos 1999; Kharaka and Hanor 2004; Cacace et al. 2010; Stober and Bucher 2013). Salinity in geothermal fluids is defined by all fluid solutes and may vary significantly across scales. It originates from a number of complex and partly interacting processes which can include the dissolution of various minerals, ion exchanges, and mixing of waters from different sources and/or depths. Consequently, for different hydrogeological settings, the sources of salinity can be very different. Under certain lithostratigraphic circumstances, the contact of water with evaporite minerals such as halite and gypsum may yield very high fluid salinity.

Depending on the composition of the fluid and the total salt content, the density of the fluid changes. Moreover, deep geothermal systems display large variations in fluid salinity and salt type. This requires density data to be available for a variety of physical conditions and chemical fluid compositions at particular geothermal sites. Given the complexity of natural fluid composition, it is suggested to systematically collect data for the dominant salts in solution (i.e., NaCl, $CaCl_2$, and, to a lesser degree, KCl) as these define the density value, whereas minor fluid components, in most cases, can be neglected. However, for example, in high enthalpy geothermal systems, other species like SiO_2 and/or H_3BO_3 may become dominant and should receive further emphasis in future investigations.

In the literature, there is a wealth of data available, particularly for single (binary) salt solutions containing NaCl and KCl. Much lesser data were generated so far for $CaCl_2$ solutions, ternary systems, and elevated temperatures and pressures. This study aims to provide new data and thereby filling knowledge gaps, with a particular focus on elevated temperatures. The evaluation of the here derived analytical results profits from the data collection of Laliberté and Cooper (2004) where pure NaCl solutions are comprehensively described, some $CaCl_2$ data are contained, and the data by Zhang et al. (1997) for mixed NaCl–$CaCl_2$ solutions at 298 K are included. For pure $CaCl_2$ and mixed NaCl–$CaCl_2$ solutions, more recent publications (e.g., Safarov et al. 2005; Al Ghafri et al. 2012; Qiblawey et al. 2014; Monteiro et al. 2021; Ge and Wang 2022) can be screened for data availability and related references. To the knowledge of the authors, there are no density data available for mixed NaCl–$CaCl_2$ solutions at temperatures above 323 K (Qiblawey et al. 2014) for which this study should substantially fill data

gaps. Nonetheless, systematic repeat measurements were also performed for the pure solutions to permit checks for data quality and to assess the precision of measurements for which no comparative data are available yet.

Exploitable geothermal fluids comprise a wide range of temperature and pressure conditions that may exceed the critical temperature of water (i.e., 647 K) and pressures of 50 MPa. Due to analytical constraints, the present measurements comprise only a limited temperature range from 293 to 353 K, however, providing a sound basis for extrapolation towards higher temperatures. Measurements of density at pressures other than ambient and temperatures beyond 373 K are demanding and ongoing efforts of some of the authors beyond the scope of this study.

Chemical coupling to thermal–hydraulic–mechanical (THM) reservoir models (e.g., Kolditz et al. 2012) is becoming more and more powerful but still requires an evaluation of the predictions against analytical data. Here, an integrated study is presented that comprises both density measurements and numerical simulations on fluids of identical composition. An intercomparison of data quality is then performed between new and existing analytical results as well as the numerical density predictions. Moreover, the use of density values in TH reservoir modeling is demonstrated exemplarily by the derivation of productivity index and thermal breakthrough for a particular deep geothermal reservoir, not least to evaluate the precision to which this parameter is required for reliable predictions of these important reservoir parameters.

Overall, this study should provide the geothermal community with a new and comprehensive density data set as well as an evaluated, openly accessible, and non-empirical geochemical tool to calculate density of geothermal fluids over a wide range of physical and chemical conditions.

Experimental procedures

The density data were obtained with a commercial oscillating U-tube densitometer (Anton Paar DMA 4500M) with a stated precision of 0.00005 g/cm^3. The device was calibrated with ultrapure water at 293 K following the procedure suggested by the manufacturer. To avoid the presence of bubbles in the measuring cell, the fluid samples were heated up outside the device to 353 K. Afterwards, the respective fluid sample was injected into the preheated U-tube with a syringe. The temperature was then decreased to the respective target temperature in steps of 10 K. Data were collected after 30 min of constant density at 353 K, 343 K, 333 K, 323 K, 313 K, 303 K, 293 K, and additionally at 298 K.

Regarding the fluid samples, pure and mixed aqueous solutions of NaCl (Carl Roth GmbH+Co. KG; Sodium Chloride Cellpure) and $CaCl_2{\cdot}2H_2O$ (Carl Roth GmbH+Co. KG; Calcium Chloride Dihydrate, p.a. ACS) were prepared. Both the NaCl and the $CaCl_2{\cdot}2H_2O$ used had a purity level above 99%. The solutions were prepared by weight on a molal basis from the respective salts diluted in deionized tap water. The mixed solutions were prepared in fixed ratios of both salts related to the cations and by adding specific amounts of $CaCl_2{\cdot}2H_2O$ to the respective NaCl solution of fixed concentration. This yielded a total of 67 different fluid sample combinations in the concentration ranges of approximately 0.08 mol/kg to 6.0 mol/kg (NaCl) and 5.3 mol/kg ($CaCl_2$) as well as mixing ratios (Na^+:Ca^{2+}) of 1:0, 0:1, 1:1, 2:1, 1:2, 3:1, and 1.2:1 (Table 2). The former

six ratios were chosen for systematic reasons and the last one relates to the approximate concentration ratio of the two dominant salts in the fluid at the Groß Schönebeck, Germany, geothermal site (Regenspurg et al. 2010), exemplifying the characterization of fluid density for a particular reservoir. In contrast to pure $CaCl_2$ solutions included for comparison with existing data and related quality checks, the 1:3 mixture was not measured due to its very limited relevance in connection with natural geothermal fluids.

The precision of the analytical scale used (KERN+SOHN GmbH; model ABJ 220-4M) is 0.1 mg and the mass reproducibility is given as less than 1 ‰ relative to the weighed quantities. After the measurements, specific amounts of each sample were dried in an oven at 160 °C for several days. The respective actual molal concentration was then determined by weighing the resultant water loss to limit concentration errors that may have been introduced by the particular measurement procedure described above. This follows the approach previously taken by Wimby and Berntsson (1994).

Numerical model

The density calculations performed in this work rely on the PHREESCALE geochemical code (Lach et al. 2016, 2017). The code is an evolution of the PHREEQC software by Parkhurst and Appelo (2013) that is widely used in the geochemical modelling community. PHREEQC calculates various water properties as activity coefficients of aqueous species and water activity according to different formalisms including the Pitzer equations for concentrated aqueous electrolyte solutions (Pitzer 1991). The last version of PHREEQC (v3; https://www.usgs.gov/software/phreeqc-version-3) also includes the calculation of solution density according to the HKFmoRR (Helgeson–Kirkham–Flowers-modified-Redlich–Rosenfeld) equation to compute the partial molar volume of dissolved species. For each solute, the partial molar volume is the sum of the standard partial molar volume, calculated according to the HKF theory (Helgeson et al. 1981; Tanger and Helgeson 1988), and of the correction for nonideality, which depends on the ionic strength of the solution. In this approach, the effects of ionic strength on the partial molar volume and on the activity coefficient of the solutes are not linked formally despite they are theoretically related (Pitzer 1991). In PHREESCALE, the volume V of the solution is given by (Lach et al. 2016):

$$V = n_w V_w^o + \sum\nolimits_{i \neq w} n_i V_i^o + V^{\mathrm{ex}}, \tag{1}$$

where n_w and n_i are the number of moles of water (w) and of solute (i) in the solution, V_w^o and V_i^o are the standard partial molar volumes of water and solutes, respectively, and V^{ex} is the excess volume due to the non-ideal behavior of the concentrated aqueous solution.

V_w^o is calculated according to the equation of state of pure water developed by the International Association for the Properties of Water and Steam (IAPWS; Wagner and Pruß 2002). V_i^o are calculated according to the revised HKF equation of state for aqueous species (Helgeson et al. 1981; Tanger and Helgeson 1988). At 25 °C, the standard partial molar volumes of Ca^{2+}, $CaCl^+$, $CaCl_2^0$, and Cl^- species are -18.21, 5.55, 32.23, and 17.71 cm^3/mol, respectively (Sverjensky et al. 1997). V^{ex} is calculated by deriving the excess Gibbs energy of the solution, G^{ex}, with respect to pressure, while G^{ex} is calculated using the Pitzer equations (Pitzer 1991). This approach is thermodynamically consistent

with the calculation of the thermal properties which are also defined according to the Pitzer equations, namely, the apparent relative molar enthalpy, heat capacity, and density of complex aqueous solutions.

A thermodynamic database (André et al. 2020) is associated with the PHREESCALE code for calculating the properties of a saline fluid. Its format slightly differs from the classical PHREEQC databases released with the code, since it contains the full set of HKF parameters for ionic species and a modified temperature dependence of the specific interaction parameters (Lach et al. 2016).

In this study, the brine compositions pertain to the Na–Ca–Cl–H_2O system. For the binary NaCl–H_2O system, all the interaction parameters (binary and volumetric) are from (Lach et al. 2017). These parameters are valid for temperatures ranging between 273.15 and 523.15 K and up to the solubility limits of halite. For the binary $CaCl_2$–H_2O system, the interaction parameters are taken from Lassin and André (2023) who considered the partial dissociation of the $CaCl_2$ electrolyte. In a first approximation, it is assumed that the volumetric parameters proposed by Lach et al. (2017) for the hypothetically fully dissociated electrolyte can be used, since they were determined for salinities larger than the concentration range of interest. Besides, the model developed by Lassin and André (2023) is also able to describe salt solubility in the ternary NaCl–$CaCl_2$–H_2O system over the whole range of mixture ratios, at least up to 403 K. To compare the experimental and numerical results, the standard deviation of density σ_ρ is calculated according to

$$\sigma_\rho = \sqrt{\frac{\sum \left(\rho^{\mathrm{exp}} - \rho^{\mathrm{calc}}\right)^2}{N}}, \tag{2}$$

where N is the number of values and exp and calc superscripts stand for experimental and calculated densities, ρ, respectively.

Results and discussion

All information on the fluid sample composition as well as all analytical and numerical results are compiled in the Appendix in Table 2.

In the following, selected results are displayed graphically to illustrate the dependence of density on temperature, concentration and the salt mixing ratio and to compare the analytical results with existing data and the numerical predictions.

The binary NaCl–H_2O system

This chemical system has already been extensively studied in the literature, and in Fig. 1, the density data compilation of Laliberté and Cooper (2004) at 298 K is displayed as a function of molal NaCl concentration approximately up to saturation. One notices that the density values of this study are in fair agreement but are up to 1% higher than, both, existing ones and those numerically predicted. This applies to most of all here acquired data at the respective conditions (Table 2). Potential sources of error will be discussed in "Analytical and numerical data quality". The standard deviation of density, σ_ρ, (Eq. 2) is

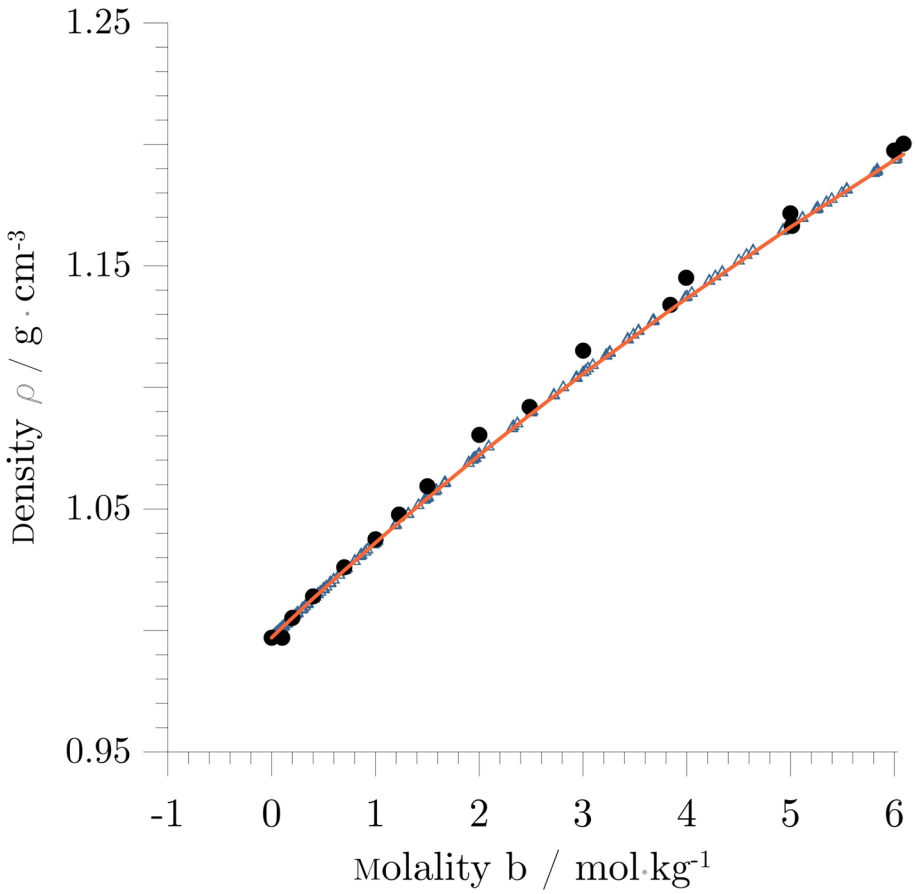

Fig. 1 Density as a function of molality for binary NaCl solutions at 298 K. Measured data (black dots) are compared with data from Laliberté and Cooper (2004; triangles) as well as the predictions of the numerical model using PHREESCALE (bold line)

calculated over a total of $N = 212$ experimental values (including the data from Laliberté and Cooper (2004) and this study) and is 0.00135 g/cm^3 (Table 2).

Figure 2 shows analytical and numerical density as function of temperature between 293 and 353 K for five different NaCl concentrations, again, in good agreement. The figure highlights the increase in density with salt concentration and its decrease with increasing temperature at constant pressure. Here, the calculated standard deviation of density is $\sigma_\rho = 0.00269$ g/cm^3 (Table 1) calculated with the 40 measured values.

The binary $CaCl_2$–H_2O system

As before, Fig. 3 displays the density data compilation of Laliberté and Cooper (2004) at 298 K as a function of molal $CaCl_2$ concentration approximately up to saturation. As for the NaCl system, the quality of the original data is good. With the numerical model the measured densities for the $CaCl_2$–H_2O system can be reproduced up to about 6 mol/kg. Thereby it is confirmed that optimized volumetric interaction parameters are not necessary for calculations in this concentration range. Beyond, the model overestimates

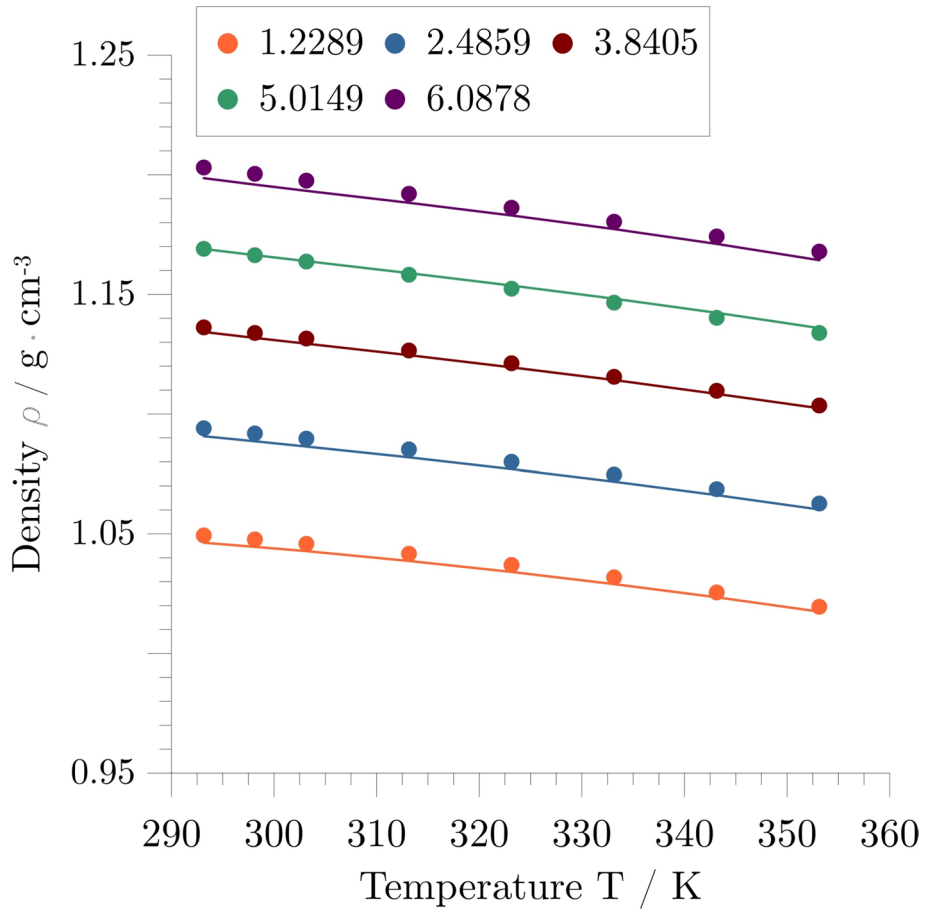

Fig. 2 Density as a function of temperature for binary NaCl solutions and five different concentrations. Measured data (dots) are compared with the predictions of the numerical model using PHREESCALE (lines). Numbers in the legend indicate molal concentration in mol/kg

Table 1 Comparison of the density standard deviations σ_ρ for the two binary and the ternary systems

Chemical system	Temperature range (K)	Literature data		This study		Global	
		N	σ_ρ (g/cm^3)	*N*	σ_ρ (g/cm^3)	*N*	σ_ρ (g/cm^3)
NaCl–H_2O	298	195	0.00026	17	0.00470	212	0.00135
NaCl–H_2O	293–353	454	0.00025	40	0.00269	494	0.00080
$CaCl_2$–H_2O	298	148	0.00696	13	0.02647	161	0.01006
$CaCl_2$–H_2O	293–353	311	0.01649	40	0.01023	351	0.01590
NaCl–$CaCl_2$–H_2O	293–353	205	0.00096	280	0.00653	485	0.00500

Literature data refer to the compilation of Laliberté and Cooper (2004) and *N* indicates the respective number of density values

the true solution density. This overestimation of density values explains the somewhat higher value of σ_ρ (0.01006 g/cm^3; Table 2) calculated for $N = 161$ values at 298 K.

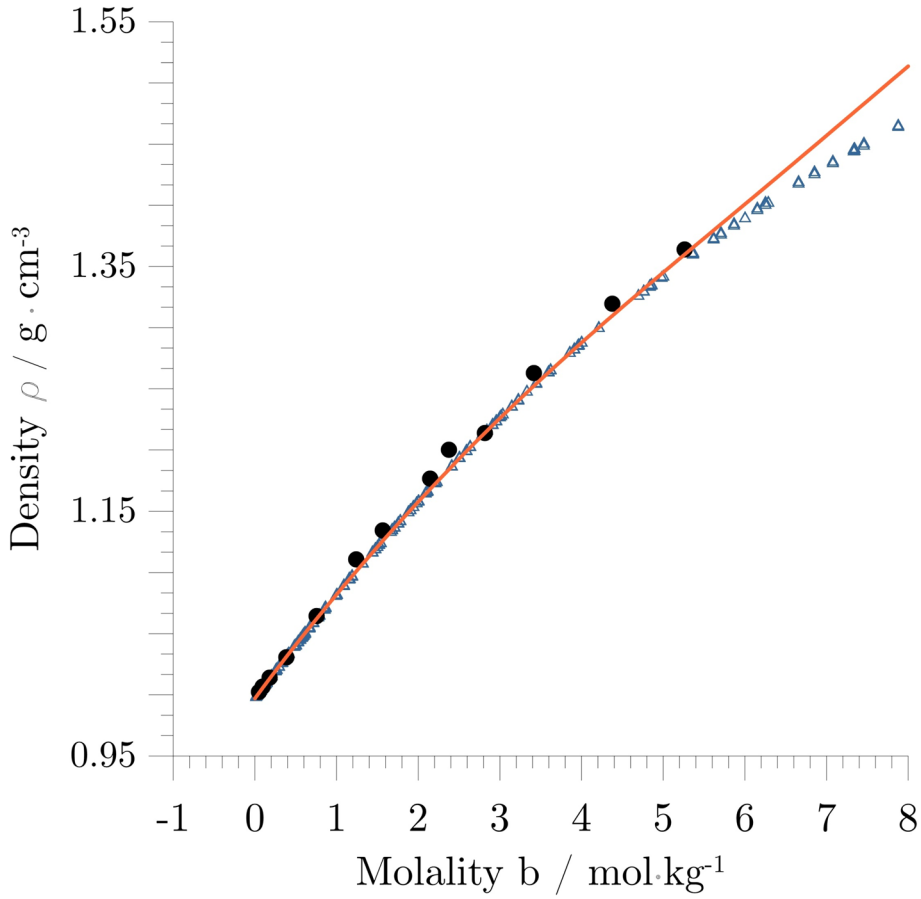

Fig. 3 Density as a function of molality for binary $CaCl_2$ solutions at 298 K. Measured data (black dots) are compared with data from Laliberté and Cooper (2004; triangles) as well as the predictions of the numerical model using PHREESCALE (bold line)

In Fig. 4**,** the variation of density for this binary system is shown as a function of temperature between 293 and 353 K and for five different $CaCl_2$ concentrations. Again, density increases with salt concentration and decreases with increasing temperature at constant pressure, as expected. The standard deviation here is $\sigma_\rho = 0.01023$ g/cm^3 (Table 2) calculated for the 40 analytical density values in this figure.

The ternary NaCl–$CaCl_2$–H_2O system

In this study, 280 new density values for mixed NaCl–$CaCl_2$ solutions were produced in the temperature range between 293 and 353 K and for Na^+:Ca^{2+} mixing ratios in the solutions of 1:2, 1:1, 1.2:1, 2:1, and 3:1.

To illustrate the relative effect of different mixing ratios in comparison to the pure solutions, Fig. 5 shows measured and numerical density values as a function of temperature for a certain, approximately comparable salt concentration based on the respective cation content (i.e., Na^+ and/or Ca^{2+}) only. During sample preparation it is difficult to obtain an exact match in total cation concentration for all mixing ratios. For the present example, the concentration deviates by ± 0.3292 mol/kg around an average

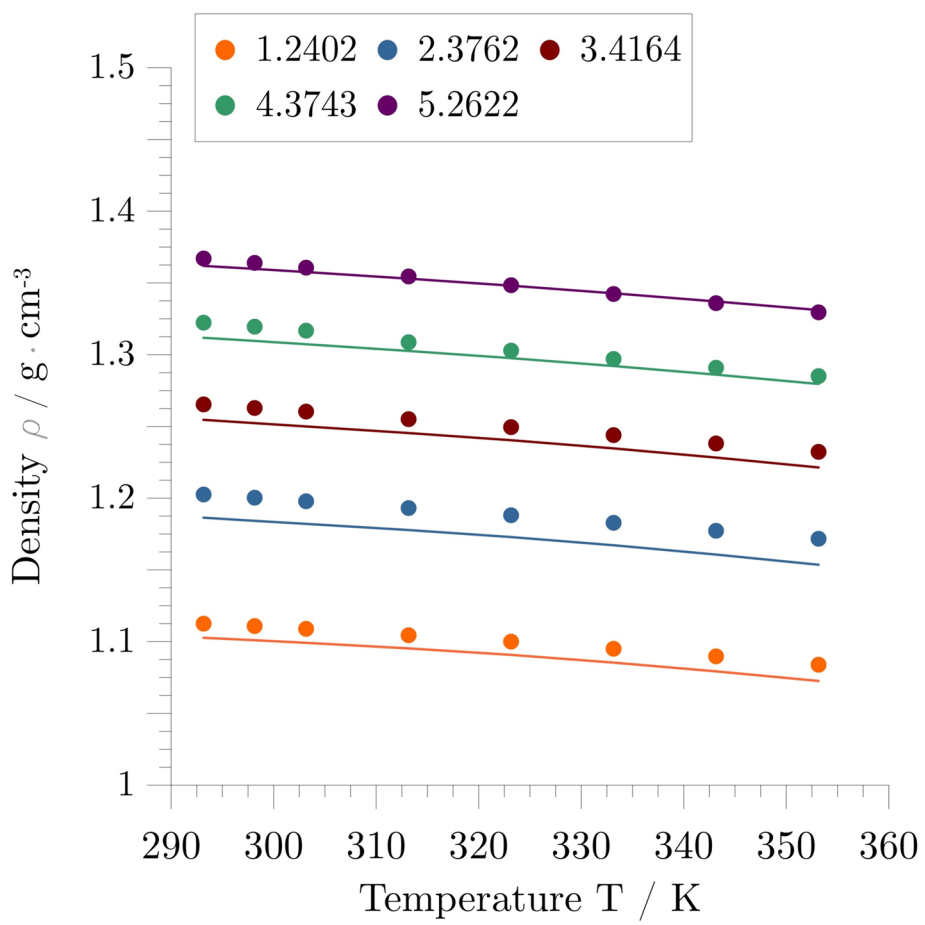

Fig. 4 Density as a function of temperature for binary $CaCl_2$ solutions and five different concentrations. Measured data (dots) are compared with the predictions of the numerical model using PHREESCALE (lines). Numbers in the legend indicate molal concentration in mol/kg

value of 3.5113 mol/kg. Apart from the expected decrease in density with increasing temperature, it can be seen that all mixtures align in parallel and their densities are in between the ones of the pure solutions. Moreover, there is a systematic increase in density with increasing Ca^{2+} content following the mixing ratio (Na^{+}:Ca^{2+}) sequence (1:0), (3:1), (2:1), (1:1), (1:2), and (0:1). Due to the differences in total cation concentration the density differences between the mixtures at a given temperature are not equidistant. Again, the match between measured and numerically calculated densities is good but variable and ranges from 0.2% (pure NaCl solution) to approximately 0.9% (at higher $CaCl_2$ content). The standard deviation for the ternary system is $\sigma_\rho = 0.00653$ g/cm^3 calculated for all 280 analytical density values acquired in this study (Table 2).

Moreover, to constrain the relative effect of different physicochemical parameters on density, also in comparison to the pure solutions, Fig. 6 displays measured and numerical density values as a function of temperature for a certain, approximately comparable salt concentration expressed by the parameter ionic strength (I), which is defined as

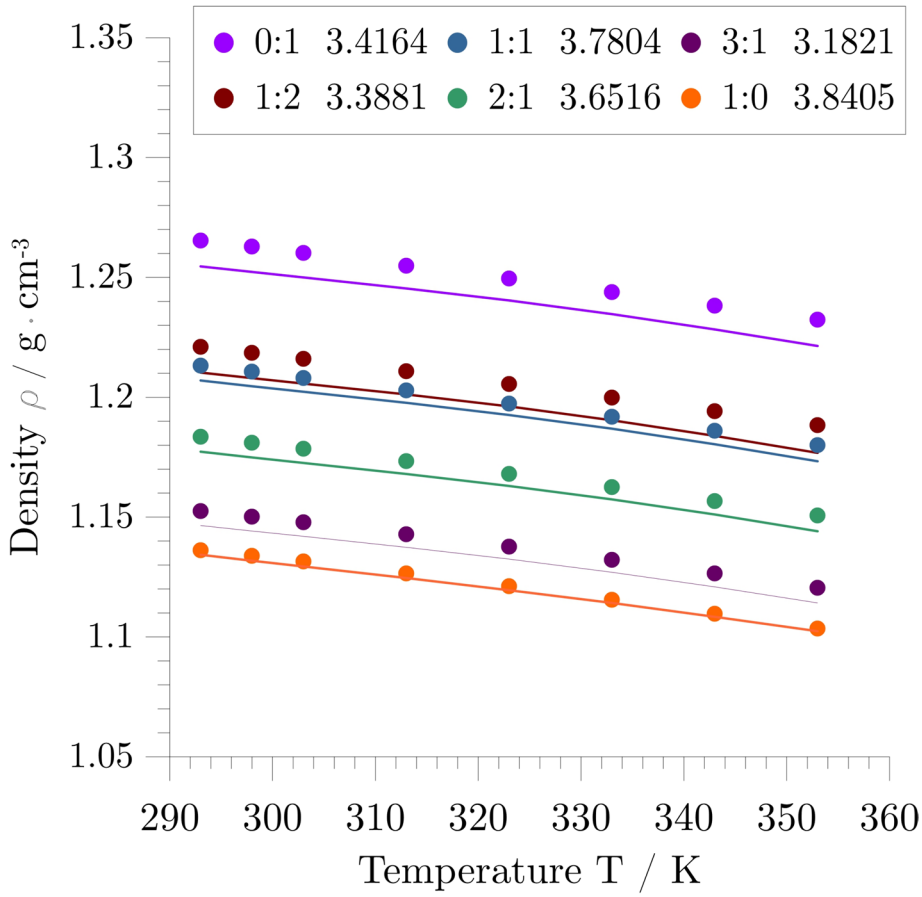

Fig. 5 Density as a function of temperature for six different mixing ratios (Na^+:$Ca.^{2+}$), i.e., (0:1) (pure $CaCl_2$), (1:0) (pure NaCl), (1:1), (2:1), (3:1), and (1:2) at total cation concentrations as indicated in the legend (i.e., 3.5113 ± 0.3292 mol/kg). Measured data (dots) are compared to the corresponding numerical model calculations using PHREESCALE (lines)

$$I = \frac{1}{2}\sum_{i=1}^{n} b_i z_i^2, \tag{3}$$

where b_i is the molality and z_i is the valence of the ion type i. It shows that, at constant temperature, density increases following the mixing ratio (Na^+:Ca^{2+}) sequence (0:1), (2:1), (1:2), (3:1), (1:1), (1.2:1), and (1:0) implying that there is no obvious systematics with ionic strength.

Older empirical mixing rules for density usually assume that the density of a ternary salt solution is the weighted sum of the densities, or apparent molal volumes, of the pure salt solutions. For most electrolytes, this is sufficient with acceptable deviation (e.g., Al Ghafri et al. 2012; Rowland and May 2018). When comparing Figs. 5 and 6, it becomes evident that density increases with Ca^{2+} concentration whereas there is obviously no such dependence on ionic strength. Dissolved ions affect the density of an

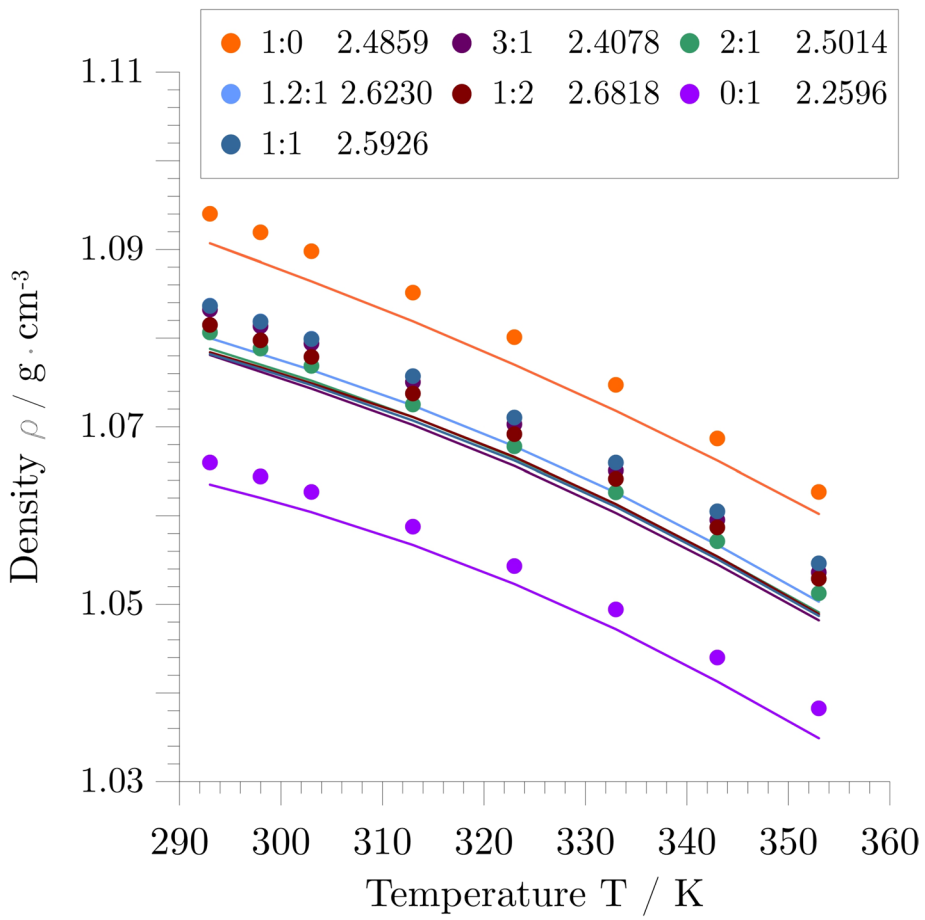

Fig. 6 Density as a function of temperature for seven different mixing ratios (Na^+:$Ca.^{2+}$), i.e., (0:1) (pure $CaCl_2$), (1:0) (pure NaCl), (1:1), (1.2:1), (2:1), (3:1), and (1:2) at total ionic strengths (Eq. 3) as indicated in the legend (i.e., 2.4707 ± 0.2111 mol/kg). Measured data (dots) are compared to the corresponding numerical model calculations using PHREESCALE (lines)

aqueous solution by their respective size, charge density, and hydration number (e.g., Falkenhagen 1971; Barthel et al. 1998). Na^+ and Ca^{2+} ions are both smaller than Cl^- ions and have a higher charge density. While Na^+ and Ca^{2+} ions are roughly of the same size, the charge density of the Ca^{2+} ion is higher. Ca^{2+} ions are therefore more dominant in the interaction with solvent molecules. While the ionic strength and the molality of NaCl are identical, the ionic strength of $CaCl_2$ is, by definition (Eq. 3), three times larger than its molality. Overall, this results in the contrasting density systematics as related to cation concentration and ionic strength of both the pure and mixed solutions.

Analytical and numerical data quality

As introduced before, Table 2 compares the standard deviation between the numerical density predictions and analytical density data, i.e., (1) compiled in Laliberté and Cooper (2004), (2) acquired in this study, and (3) for both data sets combined. For the NaCl–H_2O

system, the model reproduces the experimental data from both literature and this study with higher accuracy as compared to the $CaCl_2$–H_2O system. However, this discrepancy mainly results from the numerical overestimation of density at Ca^{2+} concentrations higher than approximately 6 mol/kg (Fig. 3). The present model could thus be improved accordingly by adjusting the speciation of calcium at very high salinities as outlined in Sect. 4.5.1. For geothermal applications this, however, is evidently of very limited relevance. Even without these modifications, the standard deviation for the ternary system is reasonable and falls between the two binary ones.

Compared to the global data collection of Laliberté and Cooper (2004), but also the data of Zhang and Han (1996), Zhang et al. (1997), and Al Ghafri et al. (2012), the measured data of this study show a larger deviation from the numerical density predictions, yielding an error band of approximately 1% as compared to typically about 0.1%. There is no evident systematic dependence on concentration, composition and temperature as the density difference appears to vary arbitrarily between samples. This makes it difficult to evidence and prioritise potential sources of errors. The precision of the densitometer claimed by the manufacturer is 0.00005 g/cm^3. To reach such a high data quality requires extreme analytical and preparative care. Any imperfection introduced during the workflow will introduce errors yielding a decrease in precision. When taking the existing data mentioned above as a reference it is intriguing that the present density values are, in most cases, slightly higher than the former. This points to a potentially inaccurate determination of concentration but rules out deficiencies in sample degassing as well as incomplete dilution. There is also the possibility that the true temperature in the U-tube is somewhat lower than measured by the temperature sensor within the device. Finally, all measurements were performed outside the calibrated density range when following the standard procedure suggested by the manufacturer. In fact, all density values acquired for pure water (Table 3) are in excellent agreement with NIST reference data (Lemmon et al. 2023). The quantification of the relative importance of all possible error sources will require more emphasis in the future. Particularly, this will yield improvements in the precise determination of the true salt concentration as well as the calibration scheme of the densitometer.

Fluid physical and geothermal implications

Numerical modeling of $CaCl_2$–H_2O density at high concentrations

The numerical approach used to calculate all the properties of the solutions is thermodynamically consistent, i.e., the speciation of dissolved species and the apparent relative molar enthalpy, heat capacity, and density of complex aqueous solutions are all assessed according to the Pitzer formalism. Indeed, the brine properties are determined from the estimation of the excess free enthalpy and its different derivatives with respect to temperature, pressure and mass of solvent. This consistency of the thermodynamic database allows to perfectly describe the properties of NaCl solutions up to the halite saturation and for a wide temperature range. However, more attention must be paid to

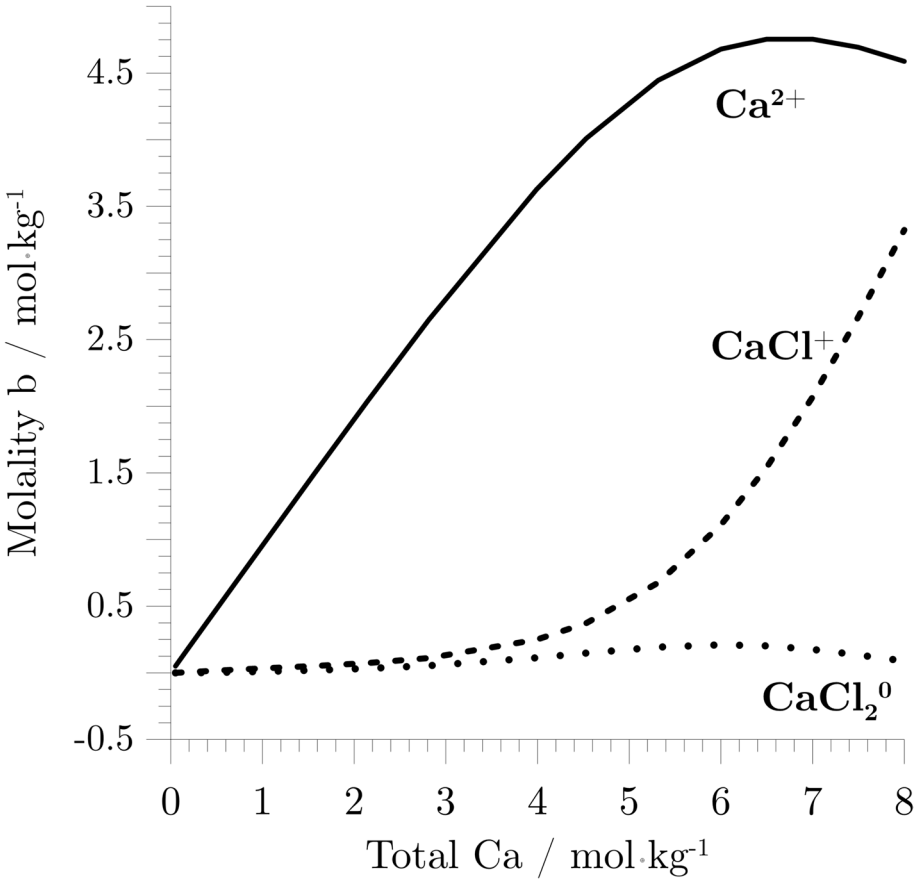

Fig. 7 Calculated aqueous speciation of the $CaCl_2$ aqueous electrolyte as a function of total Ca concentration at 298 K

the $CaCl_2$–H_2O system. Indeed, at $CaCl_2$ concentrations above approximately 6 mol/kg, the density calculations start to overestimate experimental literature data (Fig. 3; Laliberté and Cooper 2004). The aqueous speciation indicates that in this concentration range the electrolyte cannot be considered fully dissociated any longer (Fig. 7). In particular, the concentration of the $CaCl^+$ species becomes significant regarding its contribution to the volume and thus the density of the solution.

From Eq. 1, the aqueous speciation shown in Fig. 7, and the standard partial molar volumes of the various aqueous species given above, it is obvious that the contribution of $CaCl^+$ affects the calculation results in comparison with those obtained by Lach et al. (2017) who assumed full dissociation. This highlights the need for determining volumetric interaction parameters (i.e., $\beta^{(0)v}$, $\beta^{(1)v}$, and $C^{\phi v}$; e.g., Krumgalz et al. 2000) at least for the $CaCl^+$ aqueous species, to improve the calculation of density at very high concentrations. In addition, it can be expected that these volumetric interaction parameters depend on temperature. Their optimization thus requires experimental density data up

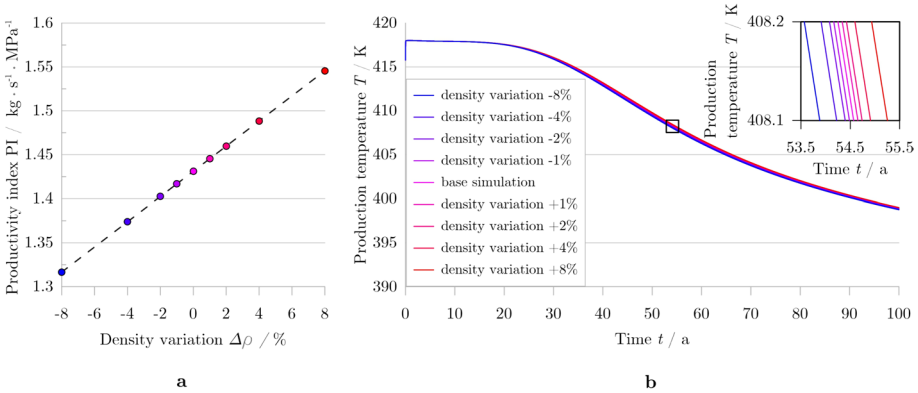

Fig. 8 Representation of the productivity index (**a**) and the timing of thermal breakthrough (**b**) for different density uncertainties during an assumed 100-year lifespan of a hydrothermal doublet for the example of the Groß Schönebeck, Germany, geothermal site (Blöcher et al. 2016)

to high concentrations at various temperatures, which is beyond the purpose of the present study.

Required density precision for geothermal reservoir modeling

To investigate the influence of density variations on key parameters of hydrothermal heat supply such as the productivity index and thermal breakthrough, a three-dimensional thermal–hydraulic (TH) reservoir simulation based on the model described by Blöcher et al. (2015) was set up with reference to the Groß Schönebeck, Germany, geothermal site (Regenspurg et al. 2010; Blöcher et al. 2016). This simulation contains the six main geological units, a production well and an injection well, as well as all hydraulically induced fractures. The latter comprise a water frac and two gel-proppant fracs on the production side and a multi-frac on the injection side. Simultaneous production and injection over a period of 100 years was simulated for a well distance in the reservoir of 500 m. The mass flow on both sides was taken as constant at a rate of 8.33 kg/s. The initial production temperature was 418 K, the injection temperature was assumed to be 343 K for all simulations and the fluid properties for the base simulation were a dynamic viscosity of 3×10^{-4} Pas and a density of 1.110 g/cm^3. To evaluate the effect of an uncertainty in density on the productivity index and the timing of thermal breakthrough, 8 additional simulations were carried out. Here, the density was assumed to deviate from the reference value stated above by − 8%, − 4%, − 2%, − 1%, + 1%, + 2%, + 4%, and + 8%, respectively. To illustrate and emphasize the particular effect of density variations all other influencing parameters were kept constant.

The results of this simulation are shown in Fig. 8. Although the mass flow rate was the same for all simulations, the volume flow rate changes with respect to the defined density. Since the volume-related productivity index, hydraulically, is an intrinsic constant of the reservoir, the different volume flow rates lead to different pressure

drawdowns, which is reflected in a change in the mass-related productivity (Fig. 8a). It shows that the so defined productivity index scales linearly with the density variations, e.g., when density is reduced by 1% this results in a 1% reduction in productivity.

Regarding the timing of thermal breakthrough, its relation to density variations is not so straight forward. For example, a lower density leads to a larger injection volume and thus would accelerate thermal breakthrough. On the other hand, a fluid with a lower density is heated more rapidly by the surrounding rock which delays thermal breakthrough. As can be seen in Fig. 8b, the first effect is dominant and a lower density leads to an acceleration of thermal breakthrough. In the present simulations, thermal breakthrough is defined as the time when the production temperature is reduced by approximately 10–408 K. For all simulations this time ranged between 53.5 and 55.5 years (Fig. 8b, insert). When addressing the analytical and/or numerical density uncertainty of the present study, a change in density by 1% leads to a change in thermal breakthrough timing by approximately 0.16% which translates into a predictive uncertainty of less than 1.5 months for an assumed duration of energetic reservoir use of 100 years.

Conclusions

530 new density values for pure and mixed NaCl–$CaCl_2$ solutions have been established by measurement. More than half of that data is unique and helps to fill existing knowledge gaps. Data quality proved fairly good and largely sufficient for geothermal applications but can be improved as evidenced by comparison with existing data. This will support future measurements expanding the physical conditions range, e.g., towards elevated pressures and higher temperatures above 373 K.

The direct comparison of the analytical data with the predictions of a thermodynamically founded numerical simulation code (i.e., PHREESCALE) is equally unique and proves the excellent predictive capabilities of this model for a wide range of chemical fluid conditions. This is of particular interest regarding the reliability of the results when coupling chemical codes to thermal–hydraulic–mechanical (THM) models for predictive large-scale geothermal reservoir modelling or other geothermal applications.

Appendix 1: Samples and data

See Table 2.

Table 2 Composition and measured as well as calculated density data (ρ) of all fluid samples at temperatures between 293 and 353 K and atmospheric pressure (0.1 MPa)

Sample	Temperature	Na (mol kgw^{-1})	Ca (mol kgw^{-1})	Cl (mol kgw^{-1})	ρ measured (g cm^{-3})	ρ calculated (g cm^{-3})	$\lvert\Delta\rho\rvert$ (%)	Ionic strength (mol kgw^{-1})
0	293	0.0000	0.0000	0.0000	0.9982	0.9982	0.0050	0.0000
1-2	293	0.1002	0.0000	0.1002	1.0031	1.0024	0.0728	0.1002
1-3	293	0.2008	0.0000	0.2008	1.0065	1.0065	0.0010	0.2008
1-4	293	0.4000	0.0000	0.4000	1.0154	1.0145	0.0897	0.4000
1-5	293	0.7013	0.0000	0.7013	1.0276	1.0263	0.1237	0.7013
1-6	293	0.9991	0.0000	0.9991	1.0392	1.0377	0.1465	0.9991
1-7	293	1.4993	0.0000	1.4993	1.0612	1.0562	0.4715	1.4993
1-8	293	2.0028	0.0000	2.0028	1.0824	1.0741	0.7709	2.0028
1-9	293	2.9997	0.0000	2.9997	1.1174	1.1077	0.8739	2.9997
1-10	293	3.9940	0.0000	3.9940	1.1475	1.1390	0.7454	3.9940
1-11	293	4.9969	0.0000	4.9969	1.1741	1.1684	0.4904	4.9969
1-12	293	5.9980	0.0000	5.9980	1.2002	1.1961	0.3436	5.9980
2-2	293	0.0000	0.0513	0.1026	1.0035	1.0029	0.0548	0.1539
2-3	293	0.0000	0.0972	0.1944	1.0081	1.0071	0.0983	0.2916
2-4	293	0.0000	0.1785	0.3570	1.0154	1.0144	0.0996	0.5355
2-5	293	0.0000	0.3828	0.7656	1.0324	1.0322	0.0203	1.1484
2-6	293	0.0000	0.7532	1.5064	1.0660	1.0635	0.2341	2.2596
2-7	293	0.0000	1.5667	3.1334	1.1363	1.1278	0.7563	4.7001
2-8	293	0.0000	2.1439	4.2878	1.1788	1.1701	0.7469	6.4317
2-9	293	0.0000	2.8150	5.6300	1.2160	1.2161	0.0049	8.4450
3-1	293	0.0855	0.0857	0.2569	1.0103	1.0095	0.0812	0.3426
3-2	293	0.3249	0.3286	0.9821	1.0416	1.0400	0.1500	1.3107
3-3	293	0.6459	0.6489	1.9437	1.0836	1.0782	0.5008	2.5926
3-4	293	1.2726	1.2662	3.8050	1.1527	1.1460	0.5812	5.0712
3-5	293	2.2426	2.2379	6.7184	1.2507	1.2384	0.9948	8.9563
4-1	293	0.3325	0.3327	0.9979	1.0439	1.0407	0.3094	1.3306
4-2	293	0.6948	0.6946	2.0840	1.0874	1.0836	0.3461	2.7786
4-3	293	0.9887	0.9869	2.9625	1.1201	1.1163	0.3386	3.9494
4-4	293	1.2670	1.2640	3.7950	1.1530	1.1457	0.6398	5.0590
4-5	293	1.6359	1.6327	4.9013	1.1912	1.1826	0.7247	6.5340
4-6	293	1.8898	1.8906	5.6710	1.2132	1.2070	0.5128	7.5616
5-1	293	0.1940	0.3875	0.9690	1.0420	1.0401	0.1846	1.3565
5-2	293	0.3832	0.7662	1.9156	1.0815	1.0784	0.2847	2.6818
5-3	293	0.5897	1.1779	2.9455	1.1253	1.1177	0.6800	4.1234
5-4	293	0.7669	1.5342	3.8353	1.1562	1.1498	0.5549	5.3695
5-5	293	0.9491	1.8987	4.7465	1.1901	1.1810	0.7663	6.6452
5-6	293	1.1296	2.2585	5.6466	1.2211	1.2103	0.8890	7.9051
6-1	293	0.5005	0.2502	1.0009	1.0432	1.0400	0.3077	1.2511
6-2	293	1.0005	0.5003	2.0011	1.0806	1.0788	0.1706	2.5014
6-3	293	1.4943	0.7471	2.9885	1.1194	1.1147	0.4252	3.7356
6-4	293	1.9639	0.9820	3.9279	1.1540	1.1469	0.6164	4.9099
6-5	293	2.4344	1.2172	4.8688	1.1835	1.1773	0.5241	6.0860
6-6	293	2.9041	1.4521	5.8083	1.2150	1.2060	0.7446	7.2604
7-1	293	0.6058	0.2020	1.0098	1.0426	1.0399	0.2596	1.2118
7-2	293	1.2039	0.4013	2.0065	1.0832	1.0781	0.4758	2.4078
7-3	293	1.8012	0.6004	3.0020	1.1216	1.1137	0.7049	3.6024

Table 2 (continued)

Sample	Temperature	Na (mol kgw^{-1})	Ca (mol kgw^{-1})	Cl (mol kgw^{-1})	ρ measured (g cm^{-3})	ρ calculated (g cm^{-3})	$\lvert\Delta\rho\rvert$ (%)	Ionic strength (mol kgw^{-1})
7-4	293	2.3866	0.7955	3.9776	1.1525	1.1465	0.5268	4.7731
7-5	293	2.9623	0.9875	4.9373	1.1848	1.1768	0.6773	5.9248
7-6	293	3.5288	1.1763	5.8814	1.2118	1.2050	0.5651	7.0577
8-1	293	0.3816	0.3143	1.0102	1.0452	1.0410	0.4044	1.3245
8-2	293	0.7558	0.6224	2.0006	1.0837	1.0800	0.3398	2.6230
8-3	293	1.1202	0.9225	2.9652	1.1230	1.1157	0.6579	3.8877
8-4	293	1.4716	1.2119	3.8954	1.1573	1.1483	0.7855	5.1073
8-5	293	1.8224	1.5007	4.8238	1.1891	1.1790	0.8584	6.3245
8-6	293	2.1688	1.7861	5.7410	1.2208	1.2077	1.0855	7.5271
9-1	293	1.2289	0.0000	1.2289	1.0494	1.0463	0.2925	1.2289
9-2	293	2.4859	0.0000	2.4859	1.0940	1.0907	0.3035	2.4859
9-3	293	3.8405	0.0000	3.8405	1.1363	1.1343	0.1746	3.8405
9-4	293	5.0149	0.0000	5.0149	1.1690	1.1690	0.0009	5.0149
9-5	293	6.0878	0.0000	6.0878	1.2030	1.1986	0.3688	6.0878
10-1	293	0.0000	1.2402	2.4804	1.1126	1.1027	0.9005	3.7206
10-2	293	0.0000	2.3762	4.7524	1.2025	1.1864	1.3604	7.1286
10-3	293	0.0000	3.4164	6.8328	1.2654	1.2546	0.8616	10.2492
10-4	293	0.0000	4.3743	8.7486	1.3224	1.3118	0.8103	13.1229
10-5	293	0.0000	5.2622	10.5240	1.3670	1.3619	0.3715	15.7866
0	298	0.0000	0.0000	0.0000	0.9970	0.9971	0.0040	0.0000
1-2	298	0.1002	0.0000	0.1002	0.9970	1.0012	0.4225	0.1002
1-3	298	0.2008	0.0000	0.2008	1.0052	1.0052	0.0030	0.2008
1-4	298	0.4000	0.0000	0.4000	1.0141	1.0132	0.0878	0.4000
1-5	298	0.7013	0.0000	0.7013	1.0261	1.0248	0.1239	0.7013
1-6	298	0.9991	0.0000	0.9991	1.0376	1.0361	0.1457	0.9991
1-7	298	1.4993	0.0000	1.4993	1.0594	1.0544	0.4723	1.4993
1-8	298	2.0028	0.0000	2.0028	1.0804	1.0722	0.7648	2.0028
1-9	298	2.9997	0.0000	2.9997	1.1152	1.1055	0.8738	2.9997
1-10	298	3.9940	0.0000	3.9940	1.1451	1.1365	0.7549	3.9940
1-11	298	4.9969	0.0000	4.9969	1.1716	1.1659	0.4880	4.9969
1-12	298	5.9980	0.0000	5.9980	1.1975	1.1935	0.3385	5.9980
2-2	298	0.0000	0.0513	0.1026	1.0023	1.0017	0.0559	0.1539
2-3	298	0.0000	0.0972	0.1944	1.0069	1.0059	0.0964	0.2916
2-4	298	0.0000	0.1785	0.3570	1.0141	1.0131	0.1027	0.5355
2-5	298	0.0000	0.3828	0.7656	1.0308	1.0309	0.0078	1.1484
2-6	298	0.0000	0.7532	1.5064	1.0644	1.0620	0.2279	2.2596
2-7	298	0.0000	1.5667	3.1334	1.1344	1.1260	0.7442	4.7001
2-8	298	0.0000	2.1439	4.2878	1.1767	1.1680	0.7440	6.4317
2-9	298	0.0000	2.8150	5.6300	1.2137	1.2138	0.0074	8.4450
3-1	298	0.0855	0.0857	0.2569	1.0091	1.0083	0.0764	0.3426
3-2	298	0.3249	0.3286	0.9821	1.0401	1.0386	0.1415	1.3107
3-3	298	0.6459	0.6489	1.9437	1.0818	1.0765	0.4942	2.5926
3-4	298	1.2726	1.2662	3.8050	1.1505	1.1439	0.5744	5.0712
3-5	298	2.2426	2.2379	6.7184	1.2480	1.2360	0.9709	8.9563
4-1	298	0.3325	0.3327	0.9979	1.0424	1.0392	0.3089	1.3306
4-2	298	0.6948	0.6946	2.0840	1.0855	1.0819	0.3364	2.7786
4-3	298	0.9887	0.9869	2.9625	1.1181	1.1143	0.3383	3.9494

Table 2 (continued)

Sample	Temperature	Na (mol kgw^{-1})	Ca (mol kgw^{-1})	Cl (mol kgw^{-1})	ρ measured (g cm^{-3})	ρ calculated (g cm^{-3})	$\lvert\Delta\rho\rvert$ (%)	Ionic strength (mol kgw^{-1})
4-4	298	1.2670	1.2640	3.7950	1.1508	1.1436	0.6313	5.0590
4-5	298	1.6359	1.6327	4.9013	1.1888	1.1803	0.7176	6.5340
4-6	298	1.8898	1.8906	5.6710	1.2107	1.2046	0.5039	7.5616
5-1	298	0.1940	0.3875	0.9690	1.0405	1.0386	0.1868	1.3565
5-2	298	0.3832	0.7662	1.9156	1.0797	1.0767	0.2823	2.6818
5-3	298	0.5897	1.1779	2.9455	1.1233	1.1158	0.6740	4.1234
5-4	298	0.7669	1.5342	3.8353	1.1540	1.1477	0.5515	5.3695
5-5	298	0.9491	1.8987	4.7465	1.1877	1.1788	0.7559	6.6452
5-6	298	1.1296	2.2585	5.6466	1.2186	1.2080	0.8750	7.9051
6-1	298	0.5005	0.2502	1.0009	1.0417	1.0385	0.3043	1.2511
6-2	298	1.0005	0.5003	2.0011	1.0788	1.0770	0.1690	2.5014
6-3	298	1.4943	0.7471	2.9885	1.1174	1.1127	0.4197	3.7356
6-4	298	1.9639	0.9820	3.9279	1.1517	1.1447	0.6124	4.9099
6-5	298	2.4344	1.2172	4.8688	1.1810	1.1749	0.5226	6.0860
6-6	298	2.9041	1.4521	5.8083	1.2124	1.2035	0.7378	7.2604
7-1	298	0.6058	0.2020	1.0098	1.0410	1.0384	0.2542	1.2118
7-2	298	1.2039	0.4013	2.0065	1.0814	1.0762	0.4795	2.4078
7-3	298	1.8012	0.6004	3.0020	1.1194	1.1116	0.7044	3.6024
7-4	298	2.3866	0.7955	3.9776	1.1502	1.1442	0.5279	4.7731
7-5	298	2.9623	0.9875	4.9373	1.1823	1.1744	0.6727	5.9248
7-6	298	3.5288	1.1763	5.8814	1.2105	1.2025	0.6678	7.0577
8-1	298	0.3816	0.3143	1.0102	1.0437	1.0395	0.4021	1.3245
8-2	298	0.7558	0.6224	2.0006	1.0819	1.0782	0.3404	2.6230
8-3	298	1.1202	0.9225	2.9652	1.1210	1.1137	0.6546	3.8877
8-4	298	1.4716	1.2119	3.8954	1.1551	1.1461	0.7844	5.1073
8-5	298	1.8224	1.5007	4.8238	1.1867	1.1767	0.8515	6.3245
8-6	298	2.1688	1.7861	5.7410	1.2182	1.2053	1.0736	7.5271
9-1	298	1.2289	0.0000	1.2289	1.0477	1.0446	0.2929	1.2289
9-2	298	2.4859	0.0000	2.4859	1.0920	1.0886	0.3077	2.4859
9-3	298	3.8405	0.0000	3.8405	1.1339	1.1318	0.1891	3.8405
9-4	298	5.0149	0.0000	5.0149	1.1664	1.1664	0.0017	5.0149
9-5	298	6.0878	0.0000	6.0878	1.2003	1.1959	0.3713	6.0878
10-1	298	0.0000	1.2402	2.4804	1.1108	1.1010	0.8901	3.7206
10-2	298	0.0000	2.3762	4.7524	1.2003	1.1842	1.3570	7.1286
10-3	298	0.0000	3.4164	6.8328	1.2628	1.2523	0.8417	10.2492
10-4	298	0.0000	4.3743	8.7486	1.3196	1.3096	0.7613	13.1229
10-5	298	0.0000	5.2622	10.5240	1.3639	1.3598	0.2993	15.7866
0	303	0.0000	0.0000	0.0000	0.9956	0.9957	0.0030	0.0000
1-2	303	0.1002	0.0000	0.1002	1.0005	0.9997	0.0740	0.1002
1-3	303	0.2008	0.0000	0.2008	1.0038	1.0038	0.0050	0.2008
1-4	303	0.4000	0.0000	0.4000	1.0125	1.0116	0.0880	0.4000
1-5	303	0.7013	0.0000	0.7013	1.0244	1.0232	0.1192	0.7013
1-6	303	0.9991	0.0000	0.9991	1.0358	1.0343	0.1479	0.9991
1-7	303	1.4993	0.0000	1.4993	1.0574	1.0525	0.4684	1.4993
1-8	303	2.0028	0.0000	2.0028	1.0783	1.0701	0.7672	2.0028
1-9	303	2.9997	0.0000	2.9997	1.1129	1.1032	0.8747	2.9997
1-10	303	3.9940	0.0000	3.9940	1.1426	1.1341	0.7513	3.9940

Table 2 (continued)

Sample	Temperature	Na (mol kgw^{-1})	Ca (mol kgw^{-1})	Cl (mol kgw^{-1})	ρ measured (g cm^{-3})	ρ calculated (g cm^{-3})	$\lvert\Delta\rho\rvert$ (%)	Ionic strength (mol kgw^{-1})
1-11	303	4.9969	0.0000	4.9969	1.1690	1.1634	0.4813	4.9969
1-12	303	5.9980	0.0000	5.9980	1.1948	1.1909	0.3292	5.9980
2-2	303	0.0000	0.0513	0.1026	1.0008	1.0003	0.0540	0.1539
2-3	303	0.0000	0.0972	0.1944	1.0054	1.0044	0.1025	0.2916
2-4	303	0.0000	0.1785	0.3570	1.0127	1.0116	0.1048	0.5355
2-5	303	0.0000	0.3828	0.7656	1.0317	1.0294	0.2215	1.1484
2-6	303	0.0000	0.7532	1.5064	1.0627	1.0604	0.2160	2.2596
2-7	303	0.0000	1.5667	3.1334	1.1323	1.1241	0.7330	4.7001
2-8	303	0.0000	2.1439	4.2878	1.1745	1.1660	0.7256	6.4317
2-9	303	0.0000	2.8150	5.6300	1.2113	1.2116	0.0231	8.4450
2-10	303	0.0000	3.9883	7.9766	1.2598	1.2847	1.9398	11.9649
2-11	303	0.0000	4.5321	9.0642	1.2969	1.3164	1.4813	13.5963
2-12	303	0.0000	5.3152	10.6300	1.3391	1.3606	1.5780	15.9456
3-1	303	0.0855	0.0857	0.2569	1.0076	1.0068	0.0795	0.3426
3–2	303	0.3249	0.3286	0.9821	1.0384	1.0370	0.1340	1.3107
3-3	303	0.6459	0.6489	1.9437	1.0799	1.0747	0.4839	2.5926
3-4	303	1.2726	1.2662	3.8050	1.1482	1.1418	0.5605	5.0712
3-5	303	2.2426	2.2379	6.7184	1.2453	1.2336	0.9452	8.9563
4-1	303	0.3325	0.3327	0.9979	1.0407	1.0376	0.3007	1.3306
4-2	303	0.6948	0.6946	2.0840	1.0836	1.0800	0.3333	2.7786
4-3	303	0.9887	0.9869	2.9625	1.1160	1.1124	0.3200	3.9494
4-4	303	1.2670	1.2640	3.7950	1.1485	1.1415	0.6159	5.0590
4-5	303	1.6359	1.6327	4.9013	1.1863	1.1781	0.6977	6.5340
4-6	303	1.8898	1.8906	5.6710	1.2081	1.2023	0.4841	7.5616
5-1	303	0.1940	0.3875	0.9690	1.0389	1.0370	0.1823	1.3565
5-2	303	0.3832	0.7662	1.9156	1.0779	1.0749	0.2772	2.6818
5-3	303	0.5897	1.1779	2.9455	1.1212	1.1138	0.6680	4.1234
5-4	303	0.7669	1.5342	3.8353	1.1518	1.1456	0.5421	5.3695
5-5	303	0.9491	1.8987	4.7465	1.1853	1.1766	0.7411	6.6452
5-6	303	1.1296	2.2585	5.6466	1.2160	1.2057	0.8576	7.9051
6-1	303	0.5005	0.2502	1.0009	1.0400	1.0369	0.2941	1.2511
6-2	303	1.0005	0.5003	2.0011	1.0769	1.0752	0.1553	2.5014
6-3	303	1.4943	0.7471	2.9885	1.1152	1.1106	0.4142	3.7356
6-4	303	1.9639	0.9820	3.9279	1.1494	1.1425	0.6013	4.9099
6-5	303	2.4344	1.2172	4.8688	1.1786	1.1726	0.5083	6.0860
6-6	303	2.9041	1.4521	5.8083	1.2097	1.2012	0.7101	7.2604
7-1	303	0.6058	0.2020	1.0098	1.0393	1.0367	0.2518	1.2118
7-2	303	1.2039	0.4013	2.0065	1.0794	1.0743	0.4729	2.4078
7-3	303	1.8012	0.6004	3.0020	1.1172	1.1095	0.6967	3.6024
7-4	303	2.3866	0.7955	3.9776	1.1479	1.1420	0.5149	4.7731
7-5	303	2.9623	0.9875	4.9373	1.1798	1.1721	0.6552	5.9248
7-6	303	3.5288	1.1763	5.8814	1.2079	1.2002	0.6382	7.0577
8-1	303	0.3816	0.3143	1.0102	1.0420	1.0379	0.3921	1.3245
8-2	303	0.7558	0.6224	2.0006	1.0799	1.0764	0.3289	2.6230
8-3	303	1.1202	0.9225	2.9652	1.1188	1.1118	0.6314	3.8877
8-4	303	1.4716	1.2119	3.8954	1.1528	1.1440	0.7675	5.1073
8-5	303	1.8224	1.5007	4.8238	1.1843	1.1744	0.8396	6.3245

Table 2 (continued)

Sample	Temperature	Na (mol kgw^{-1})	Ca (mol kgw^{-1})	Cl (mol kgw^{-1})	ρ measured (g cm^{-3})	ρ calculated (g cm^{-3})	$\lvert\Delta\rho\rvert$ (%)	Ionic strength (mol kgw^{-1})
8-6	303	2.1688	1.7861	5.7410	1.2156	1.2030	1.0490	7.5271
9-1	303	1.2289	0.0000	1.2289	1.0458	1.0428	0.2886	1.2289
9-2	303	2.4859	0.0000	2.4859	1.0898	1.0864	0.3120	2.4859
9-3	303	3.8405	0.0000	3.8405	1.1315	1.1294	0.1895	3.8405
9-4	303	5.0149	0.0000	5.0149	1.1638	1.1639	0.0129	5.0149
9-5	303	6.0878	0.0000	6.0878	1.1976	1.1933	0.3620	6.0878
10-1	303	0.0000	1.2402	2.4804	1.1089	1.0992	0.8779	3.7206
10-2	303	0.0000	2.3762	4.7524	1.1980	1.1821	1.3408	7.1286
10-3	303	0.0000	3.4164	6.8328	1.2602	1.2500	0.8192	10.2492
10-4	303	0.0000	4.3743	8.7486	1.3167	1.3073	0.7183	13.1229
10-5	303	0.0000	5.2622	10.5240	1.3608	1.3576	0.2350	15.7866
0	313	0.0000	0.0000	0.0000	0.9922	0.9922	0.0020	0.0000
1-2	313	0.1002	0.0000	0.1002	1.0019	0.9962	0.5691	0.1002
1-3	313	0.2008	0.0000	0.2008	1.0006	1.0002	0.0440	0.2008
1-4	313	0.4000	0.0000	0.4000	1.0088	1.0079	0.0873	0.4000
1-5	313	0.7013	0.0000	0.7013	1.0203	1.0194	0.0844	0.7013
1-6	313	0.9991	0.0000	0.9991	1.0318	1.0304	0.1378	0.9991
1-7	313	1.4993	0.0000	1.4993	1.0532	1.0483	0.4627	1.4993
1-8	313	2.0028	0.0000	2.0028	1.0738	1.0657	0.7582	2.0028
1-9	313	2.9997	0.0000	2.9997	1.1048	1.0985	0.5699	2.9997
1-10	313	3.9940	0.0000	3.9940	1.1375	1.1292	0.7315	3.9940
1-11	313	4.9969	0.0000	4.9969	1.1636	1.1584	0.4523	4.9969
1-12	313	5.9980	0.0000	5.9980	1.1919	1.1859	0.5093	5.9980
2-2	313	0.0000	0.0513	0.1026	0.9974	0.9969	0.0512	0.1539
2-3	313	0.0000	0.0972	0.1944	1.0019	1.0010	0.0939	0.2916
2-4	313	0.0000	0.1785	0.3570	1.0091	1.0081	0.1002	0.5355
2-5	313	0.0000	0.3828	0.7656	1.0280	1.0258	0.2135	1.1484
2-6	313	0.0000	0.7532	1.5064	1.0588	1.0567	0.1968	2.2596
2-7	313	0.0000	1.5667	3.1334	1.1280	1.1201	0.7017	4.7001
2-8	313	0.0000	2.1439	4.2878	1.1698	1.1617	0.6973	6.4317
2-9	313	0.0000	2.8150	5.6300	1.2064	1.2071	0.0572	8.4450
2-10	313	0.0000	3.9883	7.9766	1.2575	1.2800	1.7547	11.9649
2-11	313	0.0000	4.5321	9.0642	1.2911	1.3117	1.5743	13.5963
2-12	313	0.0000	5.3152	10.6300	1.3332	1.3560	1.6836	15.9456
3-1	313	0.0855	0.0857	0.2569	1.0041	1.0033	0.0758	0.3426
3-2	313	0.3249	0.3286	0.9821	1.0302	1.0332	0.2933	1.3107
3-3	313	0.6459	0.6489	1.9437	1.0757	1.0707	0.4670	2.5926
3-4	313	1.2726	1.2662	3.8050	1.1434	1.1375	0.5222	5.0712
3-5	313	2.2426	2.2379	6.7184	1.2397	1.2289	0.8772	8.9563
4-1	313	0.3325	0.3327	0.9979	1.0369	1.0338	0.2960	1.3306
4-2	313	0.6948	0.6946	2.0840	1.0794	1.0760	0.3123	2.7786
4-3	313	0.9887	0.9869	2.9625	1.1114	1.1082	0.2915	3.9494
4-4	313	1.2670	1.2640	3.7950	1.1437	1.1371	0.5769	5.0590
4-5	313	1.6359	1.6327	4.9013	1.1813	1.1736	0.6518	6.5340
4-6	313	1.8898	1.8906	5.6710	1.2029	1.1977	0.4317	7.5616
5-1	313	0.1940	0.3875	0.9690	1.0351	1.0334	0.1635	1.3565
5-2	313	0.3832	0.7662	1.9156	1.0738	1.0711	0.2483	2.6818

Table 2 (continued)

Sample	Temperature	Na (mol kgw^{-1})	Ca (mol kgw^{-1})	Cl (mol kgw^{-1})	ρ measured (g cm^{-3})	ρ calculated (g cm^{-3})	$\lvert\Delta\rho\rvert$ (%)	Ionic strength (mol kgw^{-1})
5-3	313	0.5897	1.1779	2.9455	1.1168	1.1097	0.6380	4.1234
5-4	313	0.7669	1.5342	3.8353	1.1471	1.1414	0.5020	5.3695
5-5	313	0.9491	1.8987	4.7465	1.1804	1.1722	0.6953	6.6452
5-6	313	1.1296	2.2585	5.6466	1.2109	1.2012	0.8034	7.9051
6-1	313	0.5005	0.2502	1.0009	1.0360	1.0331	0.2846	1.2511
6-2	313	1.0005	0.5003	2.0011	1.0725	1.0711	0.1307	2.5014
6-3	313	1.4943	0.7471	2.9885	1.1106	1.1064	0.3787	3.7356
6-4	313	1.9639	0.9820	3.9279	1.1445	1.1380	0.5685	4.9099
6-5	313	2.4344	1.2172	4.8688	1.1734	1.1680	0.4640	6.0860
6-6	313	2.9041	1.4521	5.8083	1.2043	1.1965	0.6544	7.2604
7-1	313	0.6058	0.2020	1.0098	1.0354	1.0329	0.2401	1.2118
7-2	313	1.2039	0.4013	2.0065	1.0750	1.0702	0.4523	2.4078
7-3	313	1.8012	0.6004	3.0020	1.1125	1.1052	0.6641	3.6024
7-4	313	2.3866	0.7955	3.9776	1.1429	1.1374	0.4871	4.7731
7-5	313	2.9623	0.9875	4.9373	1.1746	1.1674	0.6142	5.9248
7-6	313	3.5288	1.1763	5.8814	1.2024	1.1954	0.5864	7.0577
8-1	313	0.3816	0.3143	1.0102	1.0381	1.0341	0.3858	1.3245
8-2	313	0.7558	0.6224	2.0006	1.0757	1.0724	0.3087	2.6230
8-3	313	1.1202	0.9225	2.9652	1.1142	1.1075	0.6059	3.8877
8-4	313	1.4716	1.2119	3.8954	1.1480	1.1396	0.7327	5.1073
8-5	313	1.8224	1.5007	4.8238	1.1792	1.1699	0.7932	6.3245
8-6	313	2.1688	1.7861	5.7410	1.2103	1.1984	0.9913	7.5271
9-1	313	1.2289	0.0000	1.2289	1.0417	1.0387	0.2859	1.2289
9-2	313	2.4859	0.0000	2.4859	1.0851	1.0819	0.2995	2.4859
9-3	313	3.8405	0.0000	3.8405	1.1265	1.1246	0.1689	3.8405
9-4	313	5.0149	0.0000	5.0149	1.1583	1.1589	0.0544	5.0149
9-5	313	6.0878	0.0000	6.0878	1.1920	1.1883	0.3147	6.0878
10-1	313	0.0000	1.2402	2.4804	1.1046	1.0953	0.8509	3.7206
10-2	313	0.0000	2.3762	4.7524	1.1931	1.1778	1.3016	7.1286
10-3	313	0.0000	3.4164	6.8328	1.2550	1.2454	0.7668	10.2492
10-4	313	0.0000	4.3743	8.7486	1.3087	1.3026	0.4714	13.1229
10-5	313	0.0000	5.2622	10.5240	1.3546	1.3530	0.1197	15.7866
0	323	0.0000	0.0000	0.0000	0.9880	0.9881	0.0030	0.0000
1-2	323	0.1002	0.0000	0.1002	0.9928	0.9920	0.0726	0.1002
1-3	323	0.2008	0.0000	0.2008	0.9964	0.9960	0.0432	0.2008
1-4	323	0.4000	0.0000	0.4000	1.0044	1.0036	0.0817	0.4000
1-5	323	0.7013	0.0000	0.7013	1.0158	1.0149	0.0877	0.7013
1-6	323	0.9991	0.0000	0.9991	1.0272	1.0258	0.1404	0.9991
1-7	323	1.4993	0.0000	1.4993	1.0484	1.0436	0.4561	1.4993
1-8	323	2.0028	0.0000	2.0028	1.0689	1.0609	0.7494	2.0028
1-9	323	2.9997	0.0000	2.9997	1.0996	1.0935	0.5533	2.9997
1-10	323	3.9940	0.0000	3.9940	1.1320	1.1241	0.7055	3.9940
1-11	323	4.9969	0.0000	4.9969	1.1581	1.1532	0.4223	4.9969
1-12	323	5.9980	0.0000	5.9980	1.1862	1.1806	0.4718	5.9980
2-2	323	0.0000	0.0513	0.1026	0.9932	0.9927	0.0514	0.1539
2-3	323	0.0000	0.0972	0.1944	0.9977	0.9968	0.0963	0.2916
2-4	323	0.0000	0.1785	0.3570	1.0049	1.0039	0.0976	0.5355

Table 2 (continued)

Sample	Temperature	Na (mol kgw^{-1})	Ca (mol kgw^{-1})	Cl (mol kgw^{-1})	ρ measured (g cm^{-3})	ρ calculated (g cm^{-3})	$\lvert\Delta\rho\rvert$ (%)	Ionic strength (mol kgw^{-1})
2-5	323	0.0000	0.3828	0.7656	1.0237	1.0215	0.2134	1.1484
2-6	323	0.0000	0.7532	1.5064	1.0543	1.0523	0.1939	2.2596
2-7	323	0.0000	1.5667	3.1334	1.1232	1.1154	0.7020	4.7001
2-8	323	0.0000	2.1439	4.2878	1.1649	1.1569	0.6898	6.4317
2-9	323	0.0000	2.8150	5.6300	1.2013	1.2021	0.0674	8.4450
2-10	323	0.0000	3.9883	7.9766	1.2521	1.2750	1.7937	11.9649
2-11	323	0.0000	4.5321	9.0642	1.2855	1.3067	1.6216	13.5963
2-12	323	0.0000	5.3152	10.6300	1.3272	1.3511	1.7719	15.9456
3-1	323	0.0855	0.0857	0.2569	0.9998	0.9991	0.0761	0.3426
3-2	323	0.3249	0.3286	0.9821	1.0302	1.0288	0.1332	1.3107
3-3	323	0.6459	0.6489	1.9437	1.0710	1.0662	0.4530	2.5926
3-4	323	1.2726	1.2662	3.8050	1.1384	1.1326	0.5112	5.0712
3-5	323	2.2426	2.2379	6.7184	1.2340	1.2238	0.8310	8.9563
4-1	323	0.3325	0.3327	0.9979	1.0324	1.0295	0.2836	1.3306
4-2	323	0.6948	0.6946	2.0840	1.0747	1.0715	0.2958	2.7786
4-3	323	0.9887	0.9869	2.9625	1.1065	1.1035	0.2728	3.9494
4-4	323	1.2670	1.2640	3.7950	1.1386	1.1323	0.5520	5.0590
4-5	323	1.6359	1.6327	4.9013	1.1760	1.1686	0.6307	6.5340
4-6	323	1.8898	1.8906	5.6710	1.1975	1.1926	0.4067	7.5616
5-1	323	0.1940	0.3875	0.9690	1.0307	1.0290	0.1652	1.3565
5-2	323	0.3832	0.7662	1.9156	1.0692	1.0666	0.2400	2.6818
5-3	323	0.5897	1.1779	2.9455	1.1120	1.1051	0.6217	4.1234
5-4	323	0.7669	1.5342	3.8353	1.1422	1.1366	0.4883	5.3695
5-5	323	0.9491	1.8987	4.7465	1.1751	1.1673	0.6716	6.6452
5-6	323	1.1296	2.2585	5.6466	1.2055	1.1962	0.7766	7.9051
6-1	323	0.5005	0.2502	1.0009	1.0316	1.0287	0.2780	1.2511
6-2	323	1.0005	0.5003	2.0011	1.0678	1.0665	0.1200	2.5014
6-3	323	1.4943	0.7471	2.9885	1.1056	1.1016	0.3658	3.7356
6-4	323	1.9639	0.9820	3.9279	1.1393	1.1331	0.5472	4.9099
6-5	323	2.4344	1.2172	4.8688	1.1681	1.1630	0.4359	6.0860
6-6	323	2.9041	1.4521	5.8083	1.1987	1.1914	0.6136	7.2604
7-1	323	0.6058	0.2020	1.0098	1.0309	1.0285	0.2314	1.2118
7-2	323	1.2039	0.4013	2.0065	1.0703	1.0656	0.4383	2.4078
7-3	323	1.8012	0.6004	3.0020	1.1075	1.1004	0.6470	3.6024
7-4	323	2.3866	0.7955	3.9776	1.1377	1.1325	0.4609	4.7731
7-5	323	2.9623	0.9875	4.9373	1.1691	1.1624	0.5798	5.9248
7-6	323	3.5288	1.1763	5.8814	1.1968	1.1903	0.5461	7.0577
8-1	323	0.3816	0.3143	1.0102	1.0336	1.0297	0.3817	1.3245
8-2	323	0.7558	0.6224	2.0006	1.0710	1.0678	0.3025	2.6230
8-3	323	1.1202	0.9225	2.9652	1.1092	1.1028	0.5831	3.8877
8-4	323	1.4716	1.2119	3.8954	1.1428	1.1347	0.7174	5.1073
8-5	323	1.8224	1.5007	4.8238	1.1739	1.1649	0.7700	6.3245
8-6	323	2.1688	1.7861	5.7410	1.2048	1.1933	0.9604	7.5271
9-1	323	1.2289	0.0000	1.2289	1.0370	1.0341	0.2804	1.2289
9-2	323	2.4859	0.0000	2.4859	1.0801	1.0770	0.2888	2.4859
9-3	323	3.8405	0.0000	3.8405	1.1212	1.1195	0.1492	3.8405
9-4	323	5.0149	0.0000	5.0149	1.1525	1.1537	0.1083	5.0149

Table 2 (continued)

Sample	Temperature	Na (mol kgw^{-1})	Ca (mol kgw^{-1})	Cl (mol kgw^{-1})	ρ measured (g cm^{-3})	ρ calculated (g cm^{-3})	$\lvert\Delta\rho\rvert$ (%)	Ionic strength (mol kgw^{-1})
9-5	323	6.0878	0.0000	6.0878	1.1863	1.1830	0.2781	6.0878
10-1	323	0.0000	1.2402	2.4804	1.1000	1.0908	0.8425	3.7206
10-2	323	0.0000	2.3762	4.7524	1.1881	1.1729	1.2942	7.1286
10-3	323	0.0000	3.4164	6.8328	1.2495	1.2404	0.7352	10.2492
10-4	323	0.0000	4.3743	8.7486	1.3029	1.2976	0.4092	13.1229
10-5	323	0.0000	5.2622	10.5240	1.3484	1.3481	0.0245	15.7866
0	333	0.0000	0.0000	0.0000	0.9832	0.9832	0.0031	0.0000
1-2	333	0.1002	0.0000	0.1002	0.9879	0.9872	0.0719	0.1002
1-3	333	0.2008	0.0000	0.2008	0.9915	0.9911	0.0404	0.2008
1-4	333	0.4000	0.0000	0.4000	0.9995	0.9987	0.0791	0.4000
1-5	333	0.7013	0.0000	0.7013	1.0108	1.0099	0.0871	0.7013
1-6	333	0.9991	0.0000	0.9991	1.0222	1.0208	0.1322	0.9991
1-7	333	1.4993	0.0000	1.4993	1.0432	1.0385	0.4487	1.4993
1-8	333	2.0028	0.0000	2.0028	1.0624	1.0557	0.6299	2.0028
1-9	333	2.9997	0.0000	2.9997	1.0941	1.0883	0.5293	2.9997
1-10	333	3.9940	0.0000	3.9940	1.1247	1.1188	0.5229	3.9940
1-11	333	4.9969	0.0000	4.9969	1.1523	1.1477	0.3999	4.9969
1-12	333	5.9980	0.0000	5.9980	1.1802	1.1749	0.4511	5.9980
2-2	333	0.0000	0.0513	0.1026	0.9884	0.9878	0.0516	0.1539
2-3	333	0.0000	0.0972	0.1944	0.9929	0.9919	0.0978	0.2916
2-4	333	0.0000	0.1785	0.3570	1.0000	0.9990	0.1001	0.5355
2-5	333	0.0000	0.3828	0.7656	1.0188	1.0165	0.2273	1.1484
2-6	333	0.0000	0.7532	1.5064	1.0494	1.0472	0.2120	2.2596
2-7	333	0.0000	1.5667	3.1334	1.1182	1.1100	0.7360	4.7001
2-8	333	0.0000	2.1439	4.2878	1.1597	1.1513	0.7296	6.4317
2-9	333	0.0000	2.8150	5.6300	1.1960	1.1964	0.0351	8.4450
2-10	333	0.0000	3.9883	7.9766	1.2464	1.2694	1.8142	11.9649
2-11	333	0.0000	4.5321	9.0642	1.2797	1.3013	1.6606	13.5963
2-12	333	0.0000	5.3152	10.6300	1.3211	1.3458	1.8368	15.9456
3-1	333	0.0855	0.0857	0.2569	0.9950	0.9942	0.0764	0.3426
3-2	333	0.3249	0.3286	0.9821	1.0252	1.0238	0.1377	1.3107
3-3	333	0.6459	0.6489	1.9437	1.0660	1.0610	0.4665	2.5926
3-4	333	1.2726	1.2662	3.8050	1.1331	1.1271	0.5288	5.0712
3-5	333	2.2426	2.2379	6.7184	1.2281	1.2180	0.8325	8.9563
4-1	333	0.3325	0.3327	0.9979	1.0275	1.0244	0.2977	1.3306
4-2	333	0.6948	0.6946	2.0840	1.0696	1.0662	0.3170	2.7786
4-3	333	0.9887	0.9869	2.9625	1.1012	1.0981	0.2859	3.9494
4-4	333	1.2670	1.2640	3.7950	1.1332	1.1268	0.5635	5.0590
4-5	333	1.6359	1.6327	4.9013	1.1705	1.1630	0.6423	6.5340
4-6	333	1.8898	1.8906	5.6710	1.1918	1.1869	0.4162	7.5616
5-1	333	0.1940	0.3875	0.9690	1.0258	1.0240	0.1738	1.3565
5-2	333	0.3832	0.7662	1.9156	1.0641	1.0613	0.2676	2.6818
5-3	333	0.5897	1.1779	2.9455	1.1068	1.0997	0.6474	4.1234
5-4	333	0.7669	1.5342	3.8353	1.1369	1.1310	0.5217	5.3695
5-5	333	0.9491	1.8987	4.7465	1.1697	1.1616	0.6939	6.6452
5-6	333	1.1296	2.2585	5.6466	1.2000	1.1904	0.8023	7.9051
6-1	333	0.5005	0.2502	1.0009	1.0266	1.0236	0.2892	1.2511

Table 2 (continued)

Sample	Temperature	Na (mol kgw^{-1})	Ca (mol kgw^{-1})	Cl (mol kgw^{-1})	ρ measured (g cm^{-3})	ρ calculated (g cm^{-3})	$\lvert\Delta\rho\rvert$ (%)	Ionic strength (mol kgw^{-1})
6-2	333	1.0005	0.5003	2.0011	1.0627	1.0613	0.1272	2.5014
6-3	333	1.4943	0.7471	2.9885	1.1003	1.0962	0.3777	3.7356
6-4	333	1.9639	0.9820	3.9279	1.1339	1.1276	0.5560	4.9099
6-5	333	2.4344	1.2172	4.8688	1.1625	1.1574	0.4406	6.0860
6-6	333	2.9041	1.4521	5.8083	1.1929	1.1857	0.6106	7.2604
7-1	333	0.6058	0.2020	1.0098	1.0259	1.0234	0.2404	1.2118
7-2	333	1.2039	0.4013	2.0065	1.0651	1.0603	0.4508	2.4078
7-3	333	1.8012	0.6004	3.0020	1.1022	1.0950	0.6548	3.6024
7-4	333	2.3866	0.7955	3.9776	1.1322	1.1270	0.4650	4.7731
7-5	333	2.9623	0.9875	4.9373	1.1635	1.1568	0.5809	5.9248
7-6	333	3.5288	1.1763	5.8814	1.1910	1.1846	0.5411	7.0577
8-1	333	0.3816	0.3143	1.0102	1.0287	1.0247	0.3865	1.3245
8-2	333	0.7558	0.6224	2.0006	1.0659	1.0626	0.3124	2.6230
8-3	333	1.1202	0.9225	2.9652	1.1039	1.0974	0.5950	3.8877
8-4	333	1.4716	1.2119	3.8954	1.1375	1.1292	0.7324	5.1073
8-5	333	1.8224	1.5007	4.8238	1.1684	1.1593	0.7815	6.3245
8-6	333	2.1688	1.7861	5.7410	1.1991	1.1876	0.9675	7.5271
9-1	333	1.2289	0.0000	1.2289	1.0319	1.0290	0.2770	1.2289
9-2	333	2.4859	0.0000	2.4859	1.0747	1.0718	0.2715	2.4859
9-3	333	3.8405	0.0000	3.8405	1.1156	1.1142	0.1230	3.8405
9-4	333	5.0149	0.0000	5.0149	1.1466	1.1482	0.1385	5.0149
9-5	333	6.0878	0.0000	6.0878	1.1804	1.1773	0.2591	6.0878
10-1	333	0.0000	1.2402	2.4804	1.0950	1.0854	0.8826	3.7206
10-2	333	0.0000	2.3762	4.7524	1.1828	1.1672	1.3382	7.1286
10-3	333	0.0000	3.4164	6.8328	1.2440	1.2347	0.7492	10.2492
10-4	333	0.0000	4.3743	8.7486	1.2970	1.2921	0.3808	13.1229
10-5	333	0.0000	5.2622	10.5240	1.3422	1.3428	0.0439	15.7866
0	343	0.0000	0.0000	0.0000	0.9777	0.9778	0.0072	0.0000
1-2	343	0.1002	0.0000	0.1002	0.9822	0.9817	0.0519	0.1002
1-3	343	0.2008	0.0000	0.2008	0.9860	0.9856	0.0406	0.2008
1-4	343	0.4000	0.0000	0.4000	0.9940	0.9932	0.0785	0.4000
1-5	343	0.7013	0.0000	0.7013	1.0053	1.0044	0.0856	0.7013
1-6	343	0.9991	0.0000	0.9991	1.0166	1.0153	0.1290	0.9991
1-7	343	1.4993	0.0000	1.4993	1.0375	1.0330	0.4385	1.4993
1-8	343	2.0028	0.0000	2.0028	1.0567	1.0502	0.6142	2.0028
1-9	343	2.9997	0.0000	2.9997	1.0883	1.0826	0.5237	2.9997
1-10	343	3.9940	0.0000	3.9940	1.1188	1.1130	0.5166	3.9940
1-11	343	4.9969	0.0000	4.9969	1.1463	1.1418	0.3932	4.9969
1-12	343	5.9980	0.0000	5.9980	1.1740	1.1687	0.4569	5.9980
2-2	343	0.0000	0.0513	0.1026	0.9875	0.9824	0.5151	0.1539
2-3	343	0.0000	0.0972	0.1944	0.9875	0.9865	0.1014	0.2916
2-4	343	0.0000	0.1785	0.3570	0.9946	0.9936	0.1087	0.5355
2-5	343	0.0000	0.3828	0.7656	1.0134	1.0110	0.2413	1.1484
2-6	343	0.0000	0.7532	1.5064	1.0440	1.0413	0.2593	2.2596
2-7	343	0.0000	1.5667	3.1334	1.1128	1.1037	0.8236	4.7001
2-8	343	0.0000	2.1439	4.2878	1.1543	1.1448	0.8272	6.4317
2-9	343	0.0000	2.8150	5.6300	1.1905	1.1900	0.0387	8.4450

Table 2 (continued)

Sample	Temperature	Na (mol kgw^{-1})	Ca (mol kgw^{-1})	Cl (mol kgw^{-1})	ρ measured (g cm^{-3})	ρ calculated (g cm^{-3})	$\lvert\Delta\rho\rvert$ (%)	Ionic strength (mol kgw^{-1})
2-10	343	0.0000	3.9883	7.9766	1.2408	1.2632	1.7756	11.9649
2-11	343	0.0000	4.5321	9.0642	1.2738	1.2953	1.6606	13.5963
2-12	343	0.0000	5.3152	10.6300	1.3150	1.3401	1.8767	15.9456
3-1	343	0.0855	0.0857	0.2569	0.9895	0.9887	0.0799	0.3426
3-2	343	0.3249	0.3286	0.9821	1.0198	1.0182	0.1532	1.3107
3-3	343	0.6459	0.6489	1.9437	1.0605	1.0551	0.5099	2.5926
3-4	343	1.2726	1.2662	3.8050	1.1275	1.1208	0.5942	5.0712
3-5	343	2.2426	2.2379	6.7184	1.2222	1.2115	0.8816	8.9563
4-1	343	0.3325	0.3327	0.9979	1.0220	1.0188	0.3151	1.3306
4-2	343	0.6948	0.6946	2.0840	1.0641	1.0603	0.3584	2.7786
4-3	343	0.9887	0.9869	2.9625	1.0957	1.0919	0.3471	3.9494
4-4	343	1.2670	1.2640	3.7950	1.1275	1.1205	0.6229	5.0590
4-5	343	1.6359	1.6327	4.9013	1.1648	1.1565	0.7142	6.5340
4-6	343	1.8898	1.8906	5.6710	1.1860	1.1804	0.4778	7.5616
5-1	343	0.1940	0.3875	0.9690	1.0204	1.0184	0.1925	1.3565
5-2	343	0.3832	0.7662	1.9156	1.0587	1.0554	0.3127	2.6818
5-3	343	0.5897	1.1779	2.9455	1.1014	1.0935	0.7179	4.1234
5-4	343	0.7669	1.5342	3.8353	1.1314	1.1247	0.5939	5.3695
5-5	343	0.9491	1.8987	4.7465	1.1640	1.1552	0.7583	6.6452
5-6	343	1.1296	2.2585	5.6466	1.1942	1.1839	0.8700	7.9051
6-1	343	0.5005	0.2502	1.0009	1.0211	1.0180	0.3035	1.2511
6-2	343	1.0005	0.5003	2.0011	1.0571	1.0554	0.1630	2.5014
6-3	343	1.4943	0.7471	2.9885	1.0948	1.0902	0.4183	3.7356
6-4	343	1.9639	0.9820	3.9279	1.1282	1.1214	0.6055	4.9099
6-5	343	2.4344	1.2172	4.8688	1.1567	1.1511	0.4882	6.0860
6-6	343	2.9041	1.4521	5.8083	1.1869	1.1792	0.6564	7.2604
7-1	343	0.6058	0.2020	1.0098	1.0204	1.0178	0.2535	1.2118
7-2	343	1.2039	0.4013	2.0065	1.0595	1.0545	0.4751	2.4078
7-3	343	1.8012	0.6004	3.0020	1.0965	1.0890	0.6905	3.6024
7-4	343	2.3866	0.7955	3.9776	1.1265	1.1209	0.4978	4.7731
7-5	343	2.9623	0.9875	4.9373	1.1577	1.1505	0.6232	5.9248
7-6	343	3.5288	1.1763	5.8814	1.1851	1.1781	0.5908	7.0577
8-1	343	0.3816	0.3143	1.0102	1.0232	1.0191	0.4033	1.3245
8-2	343	0.7558	0.6224	2.0006	1.0604	1.0567	0.3539	2.6230
8-3	343	1.1202	0.9225	2.9652	1.0985	1.0913	0.6634	3.8877
8-4	343	1.4716	1.2119	3.8954	1.1318	1.1229	0.7953	5.1073
8-5	343	1.8224	1.5007	4.8238	1.1626	1.1529	0.8440	6.3245
8-6	343	2.1688	1.7861	5.7410	1.1932	1.1811	1.0279	7.5271
9-1	343	1.2289	0.0000	1.2289	1.0256	1.0235	0.2022	1.2289
9-2	343	2.4859	0.0000	2.4859	1.0687	1.0662	0.2345	2.4859
9-3	343	3.8405	0.0000	3.8405	1.1097	1.1084	0.1164	3.8405
9-4	343	5.0149	0.0000	5.0149	1.1403	1.1423	0.1751	5.0149
9-5	343	6.0878	0.0000	6.0878	1.1743	1.1711	0.2690	6.0878
10-1	343	0.0000	1.2402	2.4804	1.0896	1.0793	0.9562	3.7206
10-2	343	0.0000	2.3762	4.7524	1.1773	1.1607	1.4328	7.1286
10-3	343	0.0000	3.4164	6.8328	1.2383	1.2283	0.8101	10.2492
10-4	343	0.0000	4.3743	8.7486	1.2910	1.2861	0.3841	13.1229

Table 2 (continued)

Sample	Temperature	Na (mol kgw^{-1})	Ca (mol kgw^{-1})	Cl (mol kgw^{-1})	ρ measured (g cm^{-3})	ρ calculated (g cm^{-3})	$\lvert\Delta\rho\rvert$ (%)	Ionic strength (mol kgw^{-1})
10-5	343	0.0000	5.2622	10.5240	1.3360	1.3371	0.0860	15.7866
0	353	0.0000	0.0000	0.0000	0.9718	0.9718	0.0041	0.0000
1-2	353	0.1002	0.0000	0.1002	0.9760	0.9758	0.0225	0.1002
1-3	353	0.2008	0.0000	0.2008	0.9801	0.9797	0.0449	0.2008
1-4	353	0.4000	0.0000	0.4000	0.9881	0.9873	0.0800	0.4000
1-5	353	0.7013	0.0000	0.7013	0.9993	0.9985	0.0831	0.7013
1-6	353	0.9991	0.0000	0.9991	1.0106	1.0093	0.1328	0.9991
1-7	353	1.4993	0.0000	1.4993	1.0315	1.0270	0.4401	1.4993
1-8	353	2.0028	0.0000	2.0028	1.0465	1.0442	0.2164	2.0028
1-9	353	2.9997	0.0000	2.9997	1.0822	1.0766	0.5174	2.9997
1-10	353	3.9940	0.0000	3.9940	1.1126	1.1069	0.5131	3.9940
1-11	353	4.9969	0.0000	4.9969	1.1401	1.1354	0.4122	4.9969
1-12	353	5.9980	0.0000	5.9980	1.1678	1.1620	0.4957	5.9980
2-2	353	0.0000	0.0513	0.1026	0.9815	0.9764	0.5203	0.1539
2-3	353	0.0000	0.0972	0.1944	0.9815	0.9805	0.1051	0.2916
2-4	353	0.0000	0.1785	0.3570	0.9887	0.9875	0.1225	0.5355
2-5	353	0.0000	0.3828	0.7656	1.0076	1.0048	0.2787	1.1484
2-6	353	0.0000	0.7532	1.5064	1.0383	1.0349	0.3266	2.2596
2-7	353	0.0000	1.5667	3.1334	1.1071	1.0968	0.9400	4.7001
2-8	353	0.0000	2.1439	4.2878	1.1486	1.1377	0.9590	6.4317
2-9	353	0.0000	2.8150	5.6300	1.1848	1.1828	0.1649	8.4450
2-10	353	0.0000	3.9883	7.9766	1.2367	1.2565	1.5774	11.9649
2-11	353	0.0000	4.5321	9.0642	1.2679	1.2889	1.6301	13.5963
2-12	353	0.0000	5.3152	10.6300	1.3087	1.3342	1.9105	15.9456
3-1	353	0.0855	0.0857	0.2569	0.9836	0.9827	0.0875	0.3426
3-2	353	0.3249	0.3286	0.9821	1.0139	1.0120	0.1858	1.3107
3-3	353	0.6459	0.6489	1.9437	1.0546	1.0487	0.5664	2.5926
3-4	353	1.2726	1.2662	3.8050	1.1216	1.1140	0.6849	5.0712
3-5	353	2.2426	2.2379	6.7184	1.2161	1.2043	0.9798	8.9563
4-1	353	0.3325	0.3327	0.9979	1.0162	1.0126	0.3516	1.3306
4-2	353	0.6948	0.6946	2.0840	1.0583	1.0538	0.4242	2.7786
4-3	353	0.9887	0.9869	2.9625	1.0900	1.0852	0.4423	3.9494
4-4	353	1.2670	1.2640	3.7950	1.1217	1.1136	0.7247	5.0590
4-5	353	1.6359	1.6327	4.9013	1.1589	1.1495	0.8143	6.5340
4-6	353	1.8898	1.8906	5.6710	1.1801	1.1733	0.5796	7.5616
5-1	353	0.1940	0.3875	0.9690	1.0145	1.0122	0.2282	1.3565
5-2	353	0.3832	0.7662	1.9156	1.0529	1.0489	0.3833	2.6818
5-3	353	0.5897	1.1779	2.9455	1.0956	1.0867	0.8153	4.1234
5-4	353	0.7669	1.5342	3.8353	1.1256	1.1177	0.7041	5.3695
5-5	353	0.9491	1.8987	4.7465	1.1584	1.1481	0.8937	6.6452
5-6	353	1.1296	2.2585	5.6466	1.1883	1.1768	0.9806	7.9051
6-1	353	0.5005	0.2502	1.0009	1.0152	1.0119	0.3232	1.2511
6-2	353	1.0005	0.5003	2.0011	1.0512	1.0491	0.2040	2.5014

Table 2 (continued)

Sample	Temperature	Na (mol kgw^{-1})	Ca (mol kgw^{-1})	Cl (mol kgw^{-1})	ρ measured (g cm^{-3})	ρ calculated (g cm^{-3})	$\lvert\Delta\rho\rvert$ (%)	Ionic strength (mol kgw^{-1})
6-3	353	1.4943	0.7471	2.9885	1.0889	1.0836	0.4854	3.7356
6-4	353	1.9639	0.9820	3.9279	1.1222	1.1146	0.6854	4.9099
6-5	353	2.4344	1.2172	4.8688	1.1507	1.1441	0.5795	6.0860
6-6	353	2.9041	1.4521	5.8083	1.1809	1.1721	0.7516	7.2604
7-1	353	0.6058	0.2020	1.0098	1.0145	1.0117	0.2718	1.2118
7-2	353	1.2039	0.4013	2.0065	1.0536	1.0482	0.5142	2.4078
7-3	353	1.8012	0.6004	3.0020	1.0906	1.0825	0.7464	3.6024
7-4	353	2.3866	0.7955	3.9776	1.1205	1.1142	0.5636	4.7731
7-5	353	2.9623	0.9875	4.9373	1.1516	1.1437	0.6934	5.9248
7-6	353	3.5288	1.1763	5.8814	1.1789	1.1711	0.6686	7.0577
8-1	353	0.3816	0.3143	1.0102	1.0172	1.0129	0.4265	1.3245
8-2	353	0.7558	0.6224	2.0006	1.0546	1.0503	0.4075	2.6230
8-3	353	1.1202	0.9225	2.9652	1.0927	1.0847	0.7348	3.8877
8-4	353	1.4716	1.2119	3.8954	1.1260	1.1161	0.8852	5.1073
8-5	353	1.8224	1.5007	4.8238	1.1567	1.1459	0.9416	6.3245
8-6	353	2.1688	1.7861	5.7410	1.1872	1.1740	1.1261	7.5271
9-1	353	1.2289	0.0000	1.2289	1.0196	1.0175	0.2025	1.2289
9-2	353	2.4859	0.0000	2.4859	1.0627	1.0602	0.2358	2.4859
9-3	353	3.8405	0.0000	3.8405	1.1036	1.1024	0.1061	3.8405
9-4	353	5.0149	0.0000	5.0149	1.1339	1.1359	0.1726	5.0149
9-5	353	6.0878	0.0000	6.0878	1.1680	1.1643	0.3144	6.0878
10-1	353	0.0000	1.2402	2.4804	1.0839	1.0726	1.0554	3.7206
10-2	353	0.0000	2.3762	4.7524	1.1716	1.1536	1.5638	7.1286
10-3	353	0.0000	3.4164	6.8328	1.2324	1.2214	0.9014	10.2492
10-4	353	0.0000	4.3743	8.7486	1.2850	1.2796	0.4197	13.1229
10-5	353	0.0000	5.2622	10.5240	1.3297	1.3311	0.1089	15.7866

$\lvert\Delta\rho\rvert$ is the absolute value of the respective density difference. Ionic strength was calculated according to **Eq.** 3. The data are arranged by increasing temperature. The sample subsets are grouped according to their respective mixing ratio, i.e., (Na^{+}:Ca^{2+})

Appendix 2: Pure water measurements

See Table 3.

Table 3 Measured density of pure water in relation to the NIST (National Institute of Standards and Technology, USA) reference data at 298 K, 313 K, and 333 K

Temperature (K)	Measured data (g cm^{-3})	NIST data	Deviation	
			Absolute ($\times$ 10^{-5})	Relative (‰)
298	0.99705	0.99705	0.03600	0.00036
313	0.99222	0.99222	0.78300	0.00789
333	0.98321	0.98320	1.47600	0.01501

Acknowledgements
The authors would like to thank Tanja Ballerstedt (GFZ) for technical assistance with the density measurements. The authors would also like to thank the reviewers for their contributions and the editor for handling the manuscript.

Author contributions
U.H. designed, managed and executed the density measurements, performed the data treatment, evaluated the results, and wrote the manuscript draft. A.L., S.G., and L.A. performed the density simulations and provided the numerical results, wrote parts of the text, and discussed the data. G.B. performed and evaluated the reservoir simulations (Sect. 4.5.2). H.M. and I.S. supervised the study, provided analytical recommendations, evaluated and discussed the data, and edited the manuscript.

Funding
Open Access funding enabled and organized by Projekt DEAL. This study has received funding from the German Federal Ministry for the Environment, Nature Conservation, Nuclear Safety and Consumer Protection (BMUV) under grant agreement no. 0325217 as well as the European Union's Horizon 2020 Research and Innovation Programme under grant agreement no. 850626. Further funding was provided by the Helmholtz Association in the framework of the national German geoscientific large-scale infrastructure project ***GeoLaB*** (https://www.geolab.kit.edu/english/index.php).

Availability of data and materials
The dataset generated during the current study is available in Appendix 1 as well as in the GFZ Data Services repository, under the following link: https://doi.org/10.5880/GFZ.4.8.2024.008.

Declarations

Competing interests
One of the co-authors (H.M.) is co-guest-editor of the special issue to which this paper has been submitted. Otherwise, the authors declare no competing interests.

Received: 24 June 2024 Accepted: 16 September 2024
Published online: 19 October 2024

References

Ahmed T. Reservoir engineering handbook. Houston: Gulf Professional Publishing; 2010. p. 1472 (**ISBN: 9780080966670**).

Al Ghafri S, Maitland GC, Trusler JPM. Densities of aqueous $MgCl_2$(aq), $CaCl_2$(aq), KI(aq), NaCl(aq), KCl(aq), $AlCl_3$(aq), and (0.964 NaCl + 0.136 KCl)(aq) at temperatures between (283 and 472) K, pressures up to 68.5 MPa, and molalities up to 6 mol·kg^{-1}. J Chem Eng Data. 2012;57(4):1288–304. https://doi.org/10.1021/je2013704.

Barthel JMG, Krienke H, Kunz W. Physical chemistry of electrolyte solutions: modern aspects. New York: Springer; 1998. p. 401 (**ISBN 3-7985-1076-8**).

Bear J. Dynamics of fluids in porous media. New York: Dover Publications; 1988. p. 764 (**ISBN: 9780486656755**).

Bethke CM, Altaner SP, Harrison WJ, Upson C. Supercomputer analysis of sedimentary basins. Science. 1988;239(4837):261–7. https://doi.org/10.1126/science.239.4837.261.

Blöcher G, Cacace M, Reinsch T, Watanabe N. Evaluation of three exploitation concepts for a deep geothermal system in the North German Basin. Comput Geosci. 2015;82:120–9. https://doi.org/10.1016/j.cageo.2015.06.005.

Blöcher G, Reinsch T, Henninges J, Milsch H, Regenspurg S, Kummerow J, Francke H, Kranz S, Saadat A, Zimmermann G, Huenges E. Hydraulic history and current state of the deep geothermal reservoir Groß Schönebeck. Geothermics. 2016;63:27–43. https://doi.org/10.1016/j.geothermics.2015.07.008.

Cacace M, Kaiser BO, Lewerenz B, Scheck-Wenderoth M. Geothermal energy in sedimentary basins: what we can learn from regional numerical models. Geochemistry. 2010;70:33–46. https://doi.org/10.1016/j.chemer.2010.05.017.

Falkenhagen H. Theorie der Elektrolyte. Stuttgart: S. Hirzel Verlag; 1971. p. 558.

Francke H, Thorade M. Density and viscosity of brine: an overview from a process engineers perspective. Geochemistry. 2010;70:23–32. https://doi.org/10.1016/j.chemer.2010.05.015.

Frick S, Regenspurg S, Kranz S, Milsch H, Saadat A, Francke H, et al. Geochemical and process engineering challenges for geothermal power generation. Chem Ing Tec. 2011;83(12):2093–104. https://doi.org/10.1002/cite.201100131.

Ge H, Wang M. Volumetric properties for the ternary system ($CaCl_2$-$SrCl_2$-H_2O) and binary sub-systems at temperatures from 278.15 K to 323.15 K. J Chem Thermodyn. 2022. https://doi.org/10.1016/j.jct.2021.106690.

Guéguen Y, Palciauskas V. Introduction to the physics of rocks. Princeton: Princeton University Press; 1994. p. 294 (**ISBN 0-691-03452**).

Helgeson HC, Kirkham DH, Flowers GC. Theoretical prediction of the thermodynamic behavior of aqueous electrolytes at high pressures and temperatures: IV. Calculation of activity coefficients, osmotic coefficients, and apparent molal and standard and relative partial molal properties to 600 C. Am J Sci. 1981;281:1249–516.

Kolditz O, Bauer S, Bilke L, et al. OpenGeoSys: an open-source initiative for numerical simulation of thermo-hydro-mechanical/chemical (THM/C) processes in porous media. Environ Earth Sci. 2012;67(2):589–99. https://doi.org/10.1007/s12665-012-1546-x.

Krumgalz BS, Pogorelskii R, Sokolov A, Pitzer KS. Volumetric ion interaction parameters for single-solute aqueous electrolyte solutions at various temperatures. J Phys Chem Ref Data. 2000;29(5):1123–40. https://doi.org/10.1063/1.1321053.

Lach A, Boulahya F, André L, Lassin A, Azaroual M, Serin JP, et al. Thermal and volumetric properties of complex aqueous electrolyte solutions using the Pitzer formalism—the PhreeSCALE code. Comput Geosci. 2016;92:58–69. https://doi.org/10.1016/j.cageo.2016.03.016.

Lach A, Ballerat-Busserolles K, André L, Simond M, Lassin A, Cézac P, et al. Experimental data and modeling of solution density and heat capacity in the Na–K–Ca–Mg–Cl–H_2O system up to 353.15 K and 5 mol·kg^{-1} ionic strength. J Chem Eng Data. 2017;62:3561–76. https://doi.org/10.1021/acs.jced.7b00553.

Laliberté M, Cooper WE. Model for calculating the density of aqueous electrolyte solutions. J Chem Eng Data. 2004;49:1141–51.

Lassin A, André L. A revised description of the binary $CaCl_2$-H_2O chemical system up to solution-mineral equilibria and temperatures of 250 °C using Pitzer equations. Extension to the multicomponent HCl-LiCl-NaCl-KCl-$MgCl_2$-$CaCl_2$-H_2O system. J Chem Thermodynamics. 2023. https://doi.org/10.1016/j.jct.2022.106927.

Lemmon EW, Bell IH, Huber ML, McLinden MO. Thermophysical properties of fluid systems. In: Linstrom PJ, Mallard WG, editors. NIST chemistry webbook, NIST standard reference database number 69. Gaithersburg: National Institute of Standards and Technology; 2023. https://doi.org/10.18434/T4D303.

Mavko G, Mukerji T, Dvorkin J. The rock physics handbook—tools for seismic analysis of porous media. Cambridge: Cambridge University Press; 2009. p. 511. https://doi.org/10.1017/CBO9780511626753.

Monteiro MF, Moura-Neto MH, Silva ILM, Moreira LC, Silva DJ, Pereira LS, Nascimento JF, Chiavone-Filho O. Solid–liquid equilibrium, density and electrical conductivity data for water + monoethylene glycol + calcium chloride mixtures. Fluid Phase Equilib. 2021. https://doi.org/10.1016/j.fluid.2021.113177.

Nicholson K. Geothermal fluids. Heidelberg: Springer; 1993. p. 263. https://doi.org/10.1007/978-3-642-77844-5.

Pitzer KS. Activity coefficients in electrolyte solutions. Boca Raton: CRC Press; 1991. p. 542.

Qiblawey H, Arshad M, Easa A, Atilhan M. Viscosity and density of ternary solution of calcium chloride + sodium chloride + water from T = (293.15 to 323.15) K. J Chem Eng Data. 2014;59(7):2133–43. https://doi.org/10.1021/je500070k.

Raffensperger JP, Vlassopoulos D. The potential for free and mixed convection in sedimentary basins. Hydrogeol J. 1999;7(6):505–20. https://doi.org/10.1007/s100400050224.

Regenspurg S, Wiersberg T, Brandt W, Huenges E, Saadat A, Schmidt K, et al. Geochemical properties of saline geothermal fluids from the in-situ geothermal laboratory Groß Schönebeck (Germany). Geochemistry. 2010;70(3):3–12. https://doi.org/10.1016/j.chemer.2010.05.002.

Rowland D, May PM. A comparative investigation of mixing rules for property prediction in multicomponent electrolyte solutions. J Solution Chem. 2018;47:107–26. https://doi.org/10.1007/s10953-018-0710-7.

Safarov JT, Najafov GN, Shahverdiyev AN, Hassel E. (p,ρ,T) and (p_s,ρ_s,T_s) properties, and apparent molar volumes V_Φ of $CaCl_2$ (aq) at T=298.15 to 398.15 K and at pressures up to p=60 MPa. J Mol Liq. 2005;116:165–74. https://doi.org/10.1016/j.molliq.2004.07.083.

Stober I, Bucher K. Geothermal energy: from theoretical models to exploration and development. Berlin: Springer; 2013. p. 291. https://doi.org/10.1007/978-3-642-13352-7.

Sverjensky DA, Shock EL, Helgeson HC. Prediction of the thermodynamic properties of aqueous metal complexes to 1000 °C and 5 kb. Geochim Cosmochim Acta. 1997;61(7):1359–412.

Tanger JC, Helgeson HC. Calculation of the thermodynamic and transport properties of aqueous species at high pressures and temperatures: revised equations of state for the standard partial molal properties of ions and electrolytes. Am J Sci. 1988;288:19–98.

Wagner W, Pruß A. The IAPWS Formulation 1995 for the thermodynamic properties of ordinary water substance for general and scientific use. J Phys Chem Ref Data. 2002;31(2):387–535.

Wimby JM, Berntsson TS. Viscosity and density of aqueous solutions of LiBr, LiCl, $ZnBr_2$, $CaCl_2$, and $LiN0_3$. 1. Single salt solutions. J Chem Eng Data. 1994;39:68–72.

Zhang HL, Han SJ. Viscosity and density of water + sodium chloride + potassium chloride solutions at 298.15 K. J Chem Eng Data. 1996;41:516–20.

Zhang HL, Chen GH, Han SJ. Viscosity and density of H_2O + NaCl + $CaCl_2$ and H_2O + KCl + $CaCl_2$ at 298.15 K. J Chem Eng Data. 1997;42:526–30.

André L, Lassin A, Lach A.: PHREESCALE.DAT: a thermodynamic database for the PhreeSCALE software, Version 1.0. 2020. https://doi.org/10.18144/xy83-6848.

Hanor JS. Origin of saline fluids in sedimentary basins. In: Parnell J, editor. Geofluids: origin, migration and evolution of fluids in sedimentary basins. Geological Society Special Publication No 78. 1994; p. 151–74.

Kharaka YK, Hanor JS. Deep fluids in the continents: I. Sedimentary basins. In: Drever JI, Holland HD, Turekian KK, editors. Treatise on geochemistry, surface and groundwater, weathering, and soils, vol. 5. Elsevier; 2004. p. 499–540

Parkhurst DL, Appelo CAJ. Description of input and examples for PHREEQC version 3: a computer program for speciation, batch-reaction, one-dimensional transport, and inverse geochemical calculations. USGS Techniques and Methods 6-A43. 2013; Reston, VA. https://doi.org/10.3133/tm6A43.

Publisher's Note